

FROM ZERO SURGERIES TO CANDIDATES FOR EXOTIC DEFINITE FOUR-MANIFOLDS

CIPRIAN MANOLESCU AND LISA PICCIRILLO

ABSTRACT. One strategy for distinguishing smooth structures on closed 4-manifolds is to produce a knot K in S^3 that is slice in one smooth filling W of S^3 but not slice in some homeomorphic smooth filling W' . In this paper we explore how 0-surgery homeomorphisms can be used to potentially construct exotic pairs of this form. In order to systematically generate a plethora of candidates for exotic pairs, we give a fully general construction of pairs of knots with the same zero surgeries. By computer experimentation, we find 21 algebraically slice knots such that, if any of them were slice, we would obtain an exotic four-sphere. We also investigate the possibility of constructing exotic smooth structures on $\#^n \mathbb{CP}^2$ in a similar fashion.

1. INTRODUCTION

Ever since the work of Freedman [19] and Donaldson [15], the following strategy for disproving the smooth 4-dimensional Poincaré conjecture has garnered interest: Find a homotopy 4-sphere W and a knot $K \subset S^3 = \partial(W \setminus \overset{\circ}{B}{}^4)$ which bounds a smoothly embedded disk in $W \setminus \overset{\circ}{B}{}^4$ but which is not slice (in B^4). It would then follow that W is homeomorphic but not diffeomorphic to S^4 . In [18], Freedman, Gompf, Morrison and Walker explicitly attempted this strategy; for a homotopy 4-sphere from the literature they found a knot K which bounds a smooth disk in the homotopy sphere, and tried to use Rasmussen's s invariant from [43] to show that K is not slice in B^4 . The s invariant is known to be zero for slice knots, but (unlike other similar invariants [39, 29]) it is unknown whether s necessarily vanishes when K bounds a smooth disk in a homotopy 4-ball. For the example in [18], however, the s invariant was 0 and in fact the homotopy 4-sphere was proven almost immediately to be standard [4].

If one wants to more systematically pursue the strategy above, one needs a robust source of examples of knots that bound smooth disks in homotopy 4-balls. It is possible to use pairs of knots K and K' with the same 0-surgeries to produce such examples as follows: If K is slice and $S_0^3(K) \cong S_0^3(K')$, then by gluing the complement of the slice disk for K to the trace of the 0-surgery for K' , we obtain a homotopy 4-sphere W , such that K' bounds a disk in $W \setminus \overset{\circ}{B}{}^4$. If $s(K') \neq 0$, then K' is not slice and W is an exotic four-sphere.

In principle, the same idea can be used to produce examples of exotic smooth structures on $\#^n \mathbb{CP}^2$ for $n \geq 1$. The work of Freedman [19] and Donaldson [15] implies that every simply-connected, positive definite, smooth, closed 4-manifold is homeomorphic to $\#^n \mathbb{CP}^2$ for some n . It is unknown if $W = \#^n \mathbb{CP}^2$ admits exotic smooth structures. Let $W^\circ = W \setminus \overset{\circ}{B}{}^4$ and define a knot to be *H-slice* in W if it bounds a smoothly embedded nullhomologous disk in W° . If we found knots K and K' such that

$$S_0^3(K) \cong S_0^3(K'), \quad K \text{ is H-slice in } W, \quad K' \text{ is not H-slice in } W,$$

we would produce an exotic smooth structure on W . Note that we could obstruct K' from being H-slice in $\#^n \mathbb{CP}^2$ by showing that Rasmussen's s invariant satisfies $s(K') < 0$; see [35].

CM was partially supported by NSF grant DMS-2003488 and a Simons Investigator award.

LP was partially supported by NSF postdoctoral fellowship DMS-1902735 and the Max Planck Institute for Mathematics.

Techniques for constructing pairs of knots with homeomorphic n -surgeries first appeared in the late 70's, see [31, 3, 32]; for $n = 0$, see [9]. Other fundamentally distinct constructions were given in [38] and [53]. Some of these constructions always produce knots such that not only are the 0-surgeries homeomorphic, but in fact the traces are diffeomorphic [3, 32, 9]. Others of these constructions sometimes produce knots with diffeomorphic traces [2]. Producing knots with diffeomorphic traces is useful for some purposes, for example for the proof that Conway's knot is not slice [42]. But pairs of knots with the same trace are not useful for obtaining exotic structures in the manner described above, as the trace embedding lemma ([17], see Lemma 3.5) readily implies that if K is H-slice in some manifold W , then so is K' .

In this paper, in order to produce a wide selection of examples, we give a fully general framework for constructing pairs of knots with homeomorphic 0-surgeries. Our framework is based on 3-component links of the following form.

Definition 1.1. *An RBG link $L = R \cup B \cup G \subset S^3$ is a 3-component rationally framed link, with framings r, b, g respectively, such that there exist homeomorphisms $\psi_B : S^3_{r,g}(R \cup G) \rightarrow S^3$ and $\psi_G : S^3_{r,b}(R \cup B) \rightarrow S^3$ and such that $H_1(S^3_{r,b,g}(R \cup B \cup G); \mathbb{Z}) = \mathbb{Z}$.*

Theorem 1.2. *Any RBG link L has a pair of associated knots K_B and K_G and homeomorphism $\phi_L : S^3_0(K_B) \rightarrow S^3_0(K_G)$. Conversely, for any 0-surgery homeomorphism $\phi : S^3_0(K) \rightarrow S^3_0(K')$ there is an associated RBG link L_ϕ with $K_B = K'$ and $K_G = K$.*

We will explain how particular cases of RBG links recover other constructions from the literature, such as annulus twisting, dualizable patterns, and Yasui's construction. Moreover, there is a straightforward condition on the homeomorphism ϕ that guarantees that it does not extend to a homeomorphism of the corresponding traces.

A simple way to construct many RBG links is to consider the following special case: We take R to be an r -framed knot with $r \in \mathbb{Z}$, and B and G to be 0-framed unknots with linking number l such that $l = 0$ or $rl = 2$. Further, letting μ_R denote a meridian for R , we ask that there exist link isotopies

$$R \cup B \cong R \cup \mu_R \cong R \cup G.$$

We call RBG links of this form *special*. Special RBG links are easy to draw, and suffice to produce many examples of knots with the same 0-surgeries, where the corresponding traces are not homeomorphic.

Using the computer programs *SnapPy* [13], *KnotTheory* [7], *SKnotJob* [46], and the *Knot Floer homology calculator* [49], we investigated a 6-parameter family consisting of 3375 special RBG links. This yielded several interesting pairs (K, K') for which $S^3_0(K) \cong S^3_0(K')$, $s(K') = -2 \neq 0$, and for which we could not determine whether K is slice. Thus, we obtained 21 knots K with the following property.

Theorem 1.3. *If any of the 21 knots shown in Figures 22 and 23 are slice, then an exotic four-sphere exists.*

We have verified that these knots pass many of the known obstructions to sliceness. Specifically:

- They are algebraically slice (in particular, they satisfy the Fox-Milnor condition on the Alexander polynomial, and their Levine-Tristram signature function is zero);
- Their τ , ϵ and ν invariants from knot Floer homology vanish;
- Rasmussen's s invariant equals zero;
- The variants $s^{\mathbb{F}_2}$ and $s^{\mathbb{F}_3}$ of Rasmussen's invariant (from Khovanov homology over the fields \mathbb{F}_2 and \mathbb{F}_3) also vanish;
- The Lipshitz-Sarkar Sq^1 s -invariants vanish;

- For at least 12 of these knots, the given homeomorphism $\phi : S_0^3(K) \rightarrow S_0^3(K')$ does not extend to a trace diffeomorphism, so the non-sliceness of K' does not immediately obstruct K from being slice.

Furthermore, five of the knots in Figures 22 and 23 (namely, K_1 , K_3 , K_7 , K_{12} and K_{18}) have Alexander polynomial 1, and are therefore topologically slice; cf. [19]. We do not know if the others are topologically slice.

Our computer experiments produced two other knots (shown in Figure 24) which are not slice (they fail the Fox-Milnor condition) but otherwise pass the rest of the obstructions above, and have a companion knot K' with $s(K') = -2 < 0$. This leaves open the possibility that they could lead to exotic structures on $\#^n \mathbb{CP}^2$.

Theorem 1.4. *If any of the 23 knots shown in Figures 22, 23 and 24 are H-slice in $\#^n \mathbb{CP}^2$ for some n , then an exotic $\#^n \mathbb{CP}^2$ exists.*

By contrast, one can show that all these 23 knots are H-slice in $\#^n \overline{\mathbb{CP}}^2$ for some $n > 0$. Knots that are H-slice in both $\#^n \mathbb{CP}^2$ and $\#^n \overline{\mathbb{CP}}^2$ (for some n) are called *biprojectively H-slice*, or *BPH-slice*. BPH-slice knots have vanishing Tristram-Levine signature function, and satisfy $\tau = \epsilon = s = 0$; cf. [11], [35]. We observe in Section 2 that many of the small knots for which these invariants vanish can be shown to be BPH-slice.

So far we have focused on pairs of knots (K, K') with the same 0-surgery, for which we know that K' is not slice (or not H-slice in $\#^n \mathbb{CP}^2$), and we are unsure about K . We could also look at pairs (K, K') with the same 0-surgery for which we know that K is slice (or H-slice in $\#^n \mathbb{CP}^2$), and $s(K') = 0$. (If $s(K') \neq 0$, this would be a different paper.) There are plenty of such examples coming from special RBG links or from annulus twisting. In some situations, we know that K' is in fact slice, and in others we are not sure. In either case, interesting homotopy 4-spheres can be constructed using the RBG link L_ϕ from a homeomorphism $\phi : S_0^3(K) \rightarrow S_0^3(K')$. The challenge then becomes to determine whether these homotopy 4-spheres are standard. A family of examples of homotopy 4-spheres constructed by this method is shown in Figure 19.

1.1. Organization of the paper. In Section 2 we introduce BPH-slice knots and give examples. In Section 3 we present the general RBG construction and prove Theorem 1.2, and discuss when 0-surgery homeomorphisms extend to trace homeomorphisms or diffeomorphisms. In Section 4 we restrict attention to special RBG links, and introduce a concept (small RBG links) that ensures the resulting diagrams for K_B and K_G are manageable. In Section 5 we describe our computer experiments, and explain how we arrived at the knots in Figures 22, 23 and 24. In Section 6 we review how annulus twisting gives rise to 0-surgery homeomorphisms, and give examples of homotopy 4-spheres arising from this construction. Finally, in Section 7 we relate RBG links to other known ways to produce 0-surgery homeomorphisms: annulus twisting, Yasui's construction, and dualizable patterns.

1.2. Conventions. All manifolds are smooth and oriented and all homeomorphisms are orientation preserving. Boundaries are oriented with outward normal first. Slice refers to the existence of a smooth disk, and topologically slice to that of a locally flat disk. Homology has integral coefficients. The symbol ν denotes a tubular neighborhood, and U denotes the unknot.

1.3. Acknowledgements. We would like to thank the organizers of the CRM 50th Anniversary Program in Low-Dimensional Topology (Montréal, 2019), where this collaboration started. We also thank Kyle Hayden, Chuck Livingston, and Allison Miller for helpful comments on a draft of this paper. In particular, we are grateful to Kyle Hayden for pointing out that some of the homotopy 4-spheres exhibited in that draft were in fact standard.

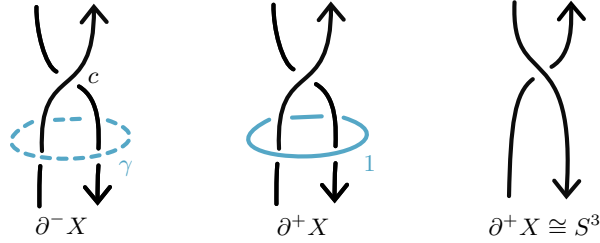


FIGURE 1. An annular cobordism in $\mathbb{CP}^2 \setminus (\overset{\circ}{B}{}^4 \sqcup \overset{\circ}{B}{}^4)$ from K to K'

2. BPH-SLICE KNOTS

Let W be a closed, smooth, oriented 4-manifold. We let $W^\circ := W \setminus \overset{\circ}{B}{}^4$.

Definition 2.1. *We say that a knot $K \subset S^3$ is H-slice in W° if it bounds a smooth, properly embedded disk Δ in W° , such that $[\Delta] = 0 \in H_2(W^\circ, \partial W^\circ)$. For convenience, we will also sometimes use the terminology H-slice in W to mean H-slice in W° .*

Observe that if a knot is slice in the usual sense, then it is H-slice in any W .

Remark 2.2. It is shown in [34, Corollary 1.5] and that the set of H-slice knots can detect exotic smooth structures on some 4-manifold with indefinite intersection form. See [34, 28] for more obstructions to H-sliceness in such manifolds.

Knots that are H-slice in some simply connected 4-manifold with a positive definite (or negative definite, resp.) intersection form are called 0-positive (0-negative, resp.) in [11]. Note that K is 0-negative iff the mirror \bar{K} is 0-positive. Several obstructions to 0-positivity are collected in [11, Proposition 1.1]. If K is 0-positive, then

- The signature of the knot satisfies $\sigma(K) \leq 0$;
- More generally, the Levine-Tristram signature function $\sigma_{LT}(K)$ (evaluated away from the roots of the Alexander polynomial) is non-positive;
- The Ozsváth-Szabó concordance invariant satisfies $\tau(K) \geq 0$; cf [39, Theorem 1.1].

There are additional obstructions from the Heegaard Floer correction terms of cyclic branched covers or ± 1 -surgeries on K , and from Yang-Mills theory; see [11], [29, Corollary 5.5] and [14, Theorem 4.1].

When $W = \#^n \mathbb{CP}^2$, another obstruction comes from Khovanov homology: From [35, Corollary 1.9], it follows that if K is H-slice in $\#^n \mathbb{CP}^2$ for some n , then Rasmussen's s invariant satisfies

$$(1) \quad s(K) \geq 0.$$

Examples of knots that are H-slice in $\#^n \mathbb{CP}^2$ can be easily constructed using the following well-known lemma.

Lemma 2.3. *Let $K, K' \subset S^3$ be knots such that K' is obtained from K by changing a negative crossing to a positive crossing in a diagram of K . If K is H-slice in $\#^{n-1} \mathbb{CP}^2$, then K' is H-slice in $\#^n \mathbb{CP}^2$.*

Proof. Let c be a negative-to-positive crossing change in a diagram of K which yields K' . Consider $K \subset S^3 \times \{0\} \subset S^3 \times I$ and attach a 1-framed 2-handle to $S^3 \times \{1\}$ along a curve γ which links c as in Figure 1. This handle attachment yields the cobordism $X = \mathbb{CP}^2 \setminus (\overset{\circ}{B}{}^4 \sqcup \overset{\circ}{B}{}^4)$ and there is a natural nullhomologous annular cobordism from $K \subset \partial^- X$ to the knot $K^+ \subset \partial^+ X$ depicted in the center frame of Figure 1. When we identify $\partial^+ X$ with the standard diagram of

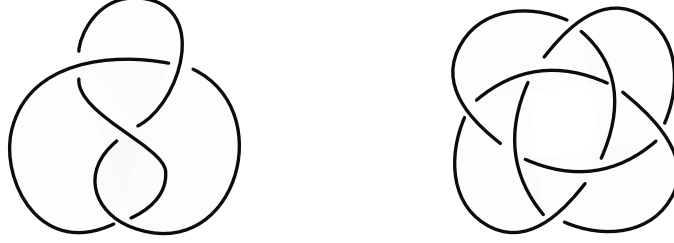


FIGURE 2. Left: the BPH-slice knot 4_1 . Right: The knot 8_{18} , whose BPH-sliceness is unknown.

S^3 (via, say, a Rolfsen twist) as in the right frame of Figure 1, we can identify K^+ as K' . The claim follows by stacking X on top of $\#^{n-1}\mathbb{CP}^2$. \square

More generally, the conclusion of Lemma 2.3 also holds when K' is obtained from K by adding a generalized positive crossing in the sense of [12, Definition 2.7].

The following concept will be of particular interest to us.

Definition 2.4. *A knot $K \subset S^3$ is called biprojectively H-slice (or BPH-slice) if it is H-slice in both $\#^n\mathbb{CP}^2$ and $\#^n\overline{\mathbb{CP}}^2$, for some $n \geq 0$.*

In [11], knots that are both 0-positive and 0-negative are called 0-bipolar. BPH-slice knots are 0-bipolar. Moreover, note that every simply connected, positive definite, smooth closed 4-manifold is homeomorphic to $\#^n\mathbb{CP}^2$ for some n , and there are no known exotic smooth structures on such manifolds. Thus, 0-bipolar and BPH-slice might be the same notion.

By applying the obstructions above for both K and \bar{K} , we see that for BPH-slice knots they become equalities instead of inequalities. Therefore, if K is BPH-slice then:

$$\sigma(K) = 0, \quad \sigma_{LT}(K) = 0, \quad \tau(K) = 0, \quad s(K) = 0.$$

Further, Hom's ϵ invariant from knot Floer homology [27] also has to vanish for BPH-slice knots; see [11, Proposition 4.10].

Slice knots are BPH-slice. We see that many of the obstructions that vanish for ordinary slice knots also vanish for BPH-slice knots. The main difference is the Fox-Milnor condition on the Alexander polynomial, which does not need to hold for BPH-slice knots.

The following is an immediate consequence of Lemma 2.3.

Lemma 2.5. *Suppose that $K \subset S^3$ is a knot with the following properties:*

- *There exists a diagram of K and a negative crossing in that diagram, such that when we change it to a positive crossing, we get a BPH-slice knot;*
- *There exists a (possibly different) diagram of K and a positive crossing in that diagram, such that when we change it to a negative crossing, we get a BPH-slice knot.*

Then, K is BPH-slice.

Example 2.6. The simplest nontrivial BPH-slice knot is the figure-eight 4_1 . Its standard diagram (shown in Figure 2) has two negative and two positive crossings, and changing the sign of any of the crossings produces the unknot.

Using Lemma 2.5, we found that BPH-slice knots are significantly more common than slice knots among small knots. Indeed, most small knots with $\sigma = 0$ are BPH-slice. Here is a list of all the prime knots with at most 9 crossings and $\sigma = 0$:

- *slice knots: $6_1, 8_8, 8_9, 8_{20}, 9_{27}, 9_{41}, 9_{46}$;*
- *amphichiral non-slice knots: $4_1, 6_3, 8_3, 8_{12}, 8_{17}, 8_{18}$;*

- *non-amphichiral, non-slice knots:* 7₇, 8₁, 8₁₃, 9₁₄, 9₁₉, 9₂₄, 9₃₀, 9₃₃, 9₃₄, 9₃₇, 9₄₄.

Of these, all except 8₁₈ can be shown to be BPH-slice by starting with the diagrams found in knot tables, checking which crossing changes produce smaller BPH-slice knots, and applying Lemma 2.5.

We could not determine if 8₁₈ is BPH-slice. Changing any of the crossings in its minimal diagram (shown in Figure 2) gives a trefoil knot, whose signature is nonzero. Observe, however, that for composite knots such as 3₁#(-3₁), it is also true that changing any crossing gives a trefoil; nevertheless, the knot is slice.

3. A GENERAL RBG CONSTRUCTION

In this section we give a fully general framework for describing homeomorphisms between manifolds arising as 0-surgeries on knots. Using this framework we discuss when a 0-surgery homeomorphism can be extended to a trace homeomorphism or diffeomorphism. In Section 4 we will make some simplifying assumptions that lead to more user-friendly results and examples.

Our construction is based on certain three-component links, called *RBG links*, which generalize those already considered in [41, Section 2].

3.1. RBG links. Let \vec{f} denote a finite ordered list with values in $\mathbb{Q} \cup \{\infty\} \cup \{\ast\}$. We will use the notation $S_{\vec{f}}^3(L)$ to denote the \vec{f} surgery on a framed link L , where an \ast denotes a complement (i.e., removing a neighborhood of that component and not filling it in). Given a 3-manifold homeomorphism $\phi : M \rightarrow N$ we will sometimes abusively still use ϕ to refer to a restriction of ϕ to some codimension zero submanifold of M .

Definition 1.1. An RBG link $L = R \cup B \cup G \subset S^3$ is a 3-component rationally framed link, with framings r, b, g respectively, such that there exist homeomorphisms $\psi_B : S_{r,g}^3(R \cup G) \rightarrow S^3$ and $\psi_G : S_{r,b}^3(R \cup B) \rightarrow S^3$ and such that $H_1(S_{r,b,g}^3(R \cup B \cup G); \mathbb{Z}) = \mathbb{Z}$.

For examples of RBG links, see Section 4.

Remark 3.1. Since there is only one orientation preserving homeomorphism of S^3 up to isotopy [10], we do not have to record the particular homeomorphisms ψ_B and ψ_G in the data of an RBG link L . We have named them in the definition for convenience in later proofs.

Theorem 1.2. Any RBG link L has a pair of associated knots K_B and K_G and homeomorphism $\phi_L : S_0^3(K_B) \rightarrow S_0^3(K_G)$. Conversely, for any 0-surgery homeomorphism $\phi : S_0^3(K) \rightarrow S_0^3(K')$ there is an associated RBG link L_ϕ with $K_B = K$ and $K_G = K'$.

Proof. For the first claim, define K_B to be the knot in S^3 satisfying $\psi_B : S_{r_*,g}^3(L) \rightarrow S^3(K_B)$ and let f_b denote the rational satisfying $\psi_B : S_{r,b,g}^3(L) \rightarrow S_{f_b}^3(K_B)$. Similarly take K_G to be the knot satisfying $\psi_G : S_{r,b,*}^3(L) \rightarrow S_*^3(K_G)$ and f_g denote the rational satisfying $\psi_B : S_{r,b,g}^3(L) \rightarrow S_{f_g}^3(K_G)$. Then $\psi_B \circ \psi_G^{-1}$ gives the desired homeomorphism ϕ_L , and the homology assumption on $S_{r,b,g}^3(L)$ implies $f_b = f_g = 0$.

For the second claim, take $B := K'$ and $b = 0$. Let μ_K be the meridian for K , and let (R, r) be the framed curve given as the image of $(\mu_K, 0)$ under the homeomorphism ϕ . Since there is the slam-dunk homeomorphism $h : S_{0,0}^3(K, \mu_K) \rightarrow S^3$, there is a homeomorphism $h \circ \phi^{-1} : S_{0,r}^3(B, R) \rightarrow S^3$. (Note that r is an integer, for homology reasons.) Now define $L = B \cup R \cup G$ where G is the 0-framed meridian of R . Observe that L is an RBG link where ψ_B is the slam dunk homeomorphism from $S_{(r,0)}^3(R, G)$ to S^3 and ψ_G is $h \circ \phi^{-1}$. \square

Remark 3.2. It is possible to produce the same 0-surgery homeomorphism from different RBG links. In the second part of Theorem 1.2 we constructed a particular RBG link, having $b = g = 0$ and $r \in \mathbb{Z}$.

There are three primary techniques presently in the literature for constructing a 0-surgery homeomorphism: dualizable patterns [3, 6, 9, 22, 32], annulus twisting [38], and Yasui's construction [53]. In Section 7 we will give explicit RBG links for each of these constructions.

3.2. H-slice knots from 0-surgery homeomorphisms. In order to build knots K' that are H-slice in an exotic copy of a simply connected four-manifold W , we will begin instead with a knot K which is H-slice in W and then construct a K' with $S_0^3(K) \cong S_0^3(K')$. That K' is then slice in a homotopy W follows from the following folklore:

Lemma 3.3. *Let W be a smooth, closed, oriented, simply connected four-manifold. If there is a homeomorphism $\phi : S_0^3(K) \rightarrow S_0^3(K')$ and K is H-slice in W , then K' is H-slice in a 4-manifold X with the homotopy type of W .*

To prove the lemma, we require a definition.

Definition 3.4. *The trace of a knot K , denoted $X(K)$, is the 4-manifold obtained by attaching a single 0-framed 2-handle to B^4 along K .*

Proof of Lemma 3.3. Since K is H-slice in W , we can choose a slice disk for K in W° and consider the 4-manifold V obtained by excising an open tubular neighborhood of that disk from W° . It is routine to confirm that $\partial V \cong S_0^3(K)$ and that $\pi_1(V)$ is normally generated by $\iota_*(\pi_1(\partial V))$, where $\iota : \partial V \rightarrow V$ is the inclusion.

Now consider the 4-manifold

$$X := X(-K') \cup_\phi V,$$

where ϕ is the assumed homeomorphism from $-\partial(X(-K')) = S_0^3(K')$ to $\partial V \cong S_0^3(K)$. Let $\mu_{K'}$ denote the meridian of K' in $S_0^3(K')$. By thinking of gluing an upside down $X(-K')$ onto a rightside up V , we see that X has a handle diagram obtained from that of V by adding an additional 0-framed 2-handle along $\phi(\mu_{K'})$, followed by a 4-handle. As such, $\pi_1(X) = \pi_1(V)/\langle[\phi(\mu_{K'})]\rangle$. Since $\pi_1(S_0^3(K'))/\langle[\mu_{K'}]\rangle = 1$ we have $\pi_1(\partial V)/\langle[\phi(\mu_{K'})]\rangle = 1$. Since $\pi_1(V)$ is normally generated by $\pi_1(\partial V)$, we have that $\pi_1(X) = 1$. It is routine to confirm that X has the homology type of W . It is then a consequence of Whitehead's Theorem (see [37, p.103, Theorem 1.5] or [23, Theorem 1.2.25]) that X is homotopy equivalent to W . (In fact, X is homeomorphic to W by Freedman's theorem [19].)

To see that K' is H-slice in X , let $X^\circ(-K')$ denote $X(-K')$ with an open ball removed, and observe that $K' \subset S^4 \subset \partial(X^\circ(-K'))$ bounds a disk D in $X^\circ(-K')$ made up of the product cobordism in $S^3 \times I$ and the core of the 2-handle. This slice disk survives into X , and it is again routine to check that $[D] = 0 \in H_2(X, \partial X)$. \square

3.3. Trace homeomorphisms. To build an exotic copy of some closed simply connected four-manifold W , we will want to start with a knot K that is H-slice in W and construct a knot K' with $S_0^3(K) \cong S_0^3(K')$ such that K' is hopefully not H-slice in W . We now observe that the following lemma implies that it is unproductive to construct a K' with the stronger property that $X(K)$ is diffeomorphic to $X(K')$:

Lemma 3.5 (Trace Embedding Lemma, originally [17], cf. [26] Lemma 3.3). *Let W be a smooth, closed 4-manifold. Then $K \subset \partial S^3$ is H-slice in W if and only if there is a smooth embedding of $X(-K)$ in W which induces the 0-map on H_2 .*

Hence, in this paper we are particularly interested in knots with homeomorphic zero-surgeries which do not have diffeomorphic traces. In full generality, it is a subtle problem to demonstrate that a pair of knot traces with homomorphic boundaries are not diffeomorphic, see [53, 25]. In fact, even the easier problem of determining whether given zero surgery homeomorphism can be extended to a trace diffeomorphism is open in general. There is some luck though: many knots have that the mapping class group of $S_0^3(K)$ is just a single element, hence if there was a trace diffeomorphism it would restrict to any given boundary homeomorphism. That $MCG(S_0^3(K)) = 1$ for a particular knot K can be verified in *SnapPy* and *Sage* [13, 47].¹

Therefore, we will be especially interested in zero-surgery homeomorphisms which do not extend to trace diffeomorphisms. First, we remind the reader that the zero-surgery homeomorphisms which do not extend to trace *homeomorphisms* are well understood:

Definition 3.6. *A 0-surgery homeomorphism $\phi : S_0^3(K) \rightarrow S_0^3(K')$ is even if the 4-manifold $Z := X(K') \cup_{\phi} -X(K)$ has even intersection form, and is odd otherwise. An RBG link is even (resp. odd) if the associated 0-surgery homeomorphism is even (resp odd).*

Theorem 3.7 ([8] Theorem 0.7 and Proposition 0.8). *A 0-surgery homeomorphism $\phi : S_0^3(K) \rightarrow S_0^3(K')$ extends to a trace homeomorphism $\Phi : X(K) \rightarrow X(K')$ if and only if ϕ is even.*

Proof. For the reader's convenience, we include a proof of the easy 'only if' direction.

Suppose for a contradiction that ϕ is not even, and that there is some homeomorphism $\Phi : X(K) \rightarrow X(K')$ extending ϕ . Let W denote the 4-manifold obtained from $X(K)$ by attaching a 0-framed 2-handle along μ_K followed by a 4-handle, and observe that W has even intersection form. Define $Z := X(K') \cup_{\phi} -X(K)$, which has odd intersection form by hypothesis. Observe that Φ gives a natural homeomorphism from W to Z , a contradiction. \square

Remark 3.8. We emphasize that Theorem 3.7 only shows that a particular boundary homeomorphism does not extend, *not* that the traces are not homeomorphic. Indeed, there are for example boundary homeomorphisms $X(U) \rightarrow X(U)$ that don't extend to trace homeomorphisms [21].

We observe that the knots whose 0-surgery admits an odd homeomorphism are somewhat restricted.

Lemma 3.9. *If a homeomorphism $\phi : S_0^3(K) \rightarrow S_0^3(K')$ is odd then $\text{Arf}(K) = \text{Arf}(K') = 0$.*

Proof. Robertello [44] showed that if X is a simply connected smooth 4-manifold with S^3 boundary and $K \subset S^3$ bounds a smooth disk D in X such that $[D] \in H_2(X, \partial X) \cong H_2(X)$ is characteristic then

$$\text{Arf}(K) = \frac{[D] \cdot [D] - \sigma(X)}{2} \bmod 2.$$

Consider the 4-manifold Z obtained by gluing $X_0(K)$ (upside down) to $X_0(K')$ (right side up) along $S_0^3(K')$ via ϕ . Remove the 0-handle of $X_0(K')$ to get X with S^3 boundary, and observe that $K' \subset S^3$ bounds a 0-framed disk D in X (the core of the 2-handle). Further, this handle decomposition of X gives a natural presentation of H_2 with basis $\{\alpha, \beta\}$ and intersection form

$$Q_X = \begin{pmatrix} 0 & 1 \\ 1 & n \end{pmatrix}.$$

Further, we see that $[D] = \alpha$ and, since n is odd, α is characteristic. Then Robertello's result applies and we get $\text{Arf}(K') = 0$. We can obtain the same conclusion about K by turning Z upside down. \square

¹*SnapPy* computes the symmetry group of a hyperbolic manifold by finding a canonical cellulation. This is done using numerical methods. If one wants a mathematical proof, then the *SnapPy* answer needs to be certified rigorously, e.g. using interval arithmetic as in [16].

Remark 3.10. The converse is false, as can be seen by considering the identity homeomorphism on $S_0^3(K)$ for any knot with $\text{Arf}(K) = 0$.

We remark that Lemma 3.9 pairs with Theorem 3.7 to demonstrate that

Corollary 3.11. *If $\text{Arf}(K) = 1$ then every 0-surgery homeomorphism $\phi : S_0^3(K) \rightarrow S_0^3(K')$ extends to a trace homeomorphism.*

3.4. Trace diffeomorphisms. It remains well out of reach to classify when 0-surgery homeomorphisms extend to trace diffeomorphisms. We give a sufficient condition for a homeomorphism to extend.

Definition 3.12. *Let $\phi : S_0^3(K) \rightarrow S_0^3(K')$ be a 0-surgery homeomorphism. Let $\gamma \subset S_0^3(K')$ be the framed knot given by the image of the 0-framed meridian of K under ϕ . We say that ϕ has property U if there is some diagrammatic choice of γ in the standard diagram of $S_0^3(K')$ where γ is 0 framed and appears unknotted in the diagram.*

Theorem 3.13. *If ϕ has property U then there exists a diffeomorphism $\Phi : X(K) \rightarrow X(K')$ with $\Phi|_{\partial} = \phi$.*

Remark 3.14. This theorem follows from a now-standard technique due to Akbulut, called carving [3], which was developed in fact exactly for this purpose. Versions of the theorem already appear in the literature; see for example [2]. Here we eliminate some hypotheses by making use of a theorem of Gabai in the last step of the proof.

Proof. Let $X \subset X(K)$ be a (closed) tubular neighborhood of the cocore disk of the 2-handle, which is naturally identified with $D^2 \times D^2$, and let $X' \subset X$ be the open neighborhood of the cocore disk, which is a $D^2 \times \mathring{D}^2$. Since the image $\phi(\mu_K)$ appears unknotted in the standard handle diagram of $X(K')$, we can identify the standard slice disk D for $\phi(\mu_K)$ in B^4 (thought of as the 0-handle). Define $Y := \nu(D) \cong D^2 \times D^2$ and $Y' \cong D^2 \times \mathring{D}^2$ similarly. Since ϕ preserves the 0-framing on μ_K , the natural bundle diffeomorphism $F' : X \rightarrow Y$ has that $F'|_{\partial(X(K))}$ agrees with $f|_{\nu(\mu_K)}$.

Let X_1 denote $X(K) \setminus X'$ and Y_1 denote $X(K') \setminus Y'$. It is evident that X_1 is diffeomorphic to B^4 . We will argue momentarily that Y_1 is also diffeomorphic to B^4 . Assuming this for now, we will finish the argument. Observe that $\phi|_{\partial X(K) \setminus \nu(\mu_K)}$ and $F'|_{D^2 \times \partial(D^2)}$ give a piecewise homeomorphism f from $\partial X_1 \cong S^3$ to $\partial Y_1 \cong S^3$. Since there is only one homeomorphism of S^3 up to isotopy [10], and it extends smoothly over B^4 , we can extend f to a diffeomorphism $F : X_1 \rightarrow Y_1$. By construction F and F' together produce a diffeomorphism from $X(K)$ to $X(K')$ extending ϕ .

Now we argue that Y_1 is diffeomorphic to B^4 . Observe that Y_1 has S^3 boundary and a handle decomposition given by dotting $\phi(\mu_K)$ in the standard handle decomposition of $X(K')$. So ∂Y_1 is naturally described as (0,0) surgery on the 2-component link $K' \cup \phi(\mu_K) \subset S^3$, and one link component is an unknot. Then, by performing the 0-surgery on $\phi(\mu_K)$ first, we can think of ∂Y_1 as S^3 obtained by surgery on some knot ℓ in $S^1 \times S^2$. By Gabai's proof of property R [20], ℓ is isotopic to $S^1 \times \{pt\}$. Performing this isotopy on the attaching sphere of our 2-handle (sliding over the 1-handle as needed) yields a handle decomposition of Y_1 which is just a canceling 1-2 pair, hence Y_1 is diffeomorphic to B^4 . \square

Question 3.15. *Is the converse of Theorem 3.13 true?*

We comment now about these properties (parity and property U) for some constructions of 0-surgery homeomorphisms from the literature. (These constructions are discussed further in Section 7.) Dualizable pattern homeomorphisms [31, 9, 22] are all even and have property U .

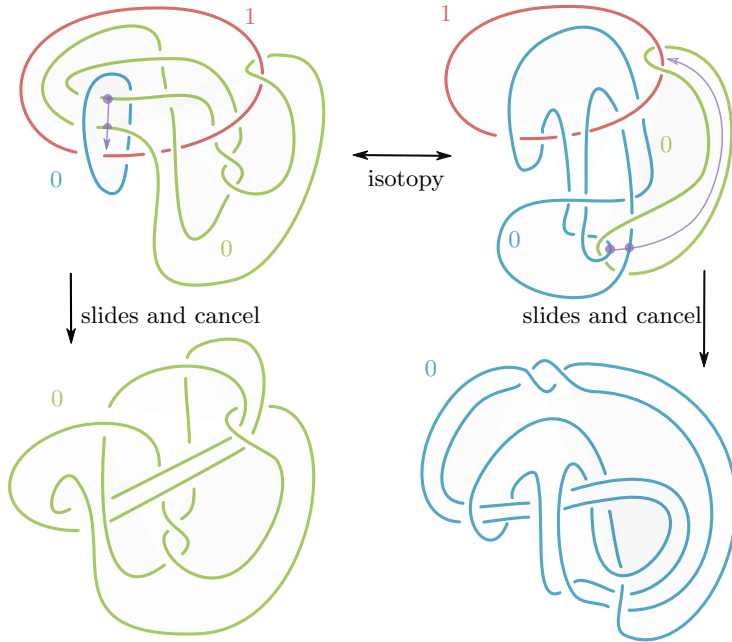


FIGURE 3. A small RBG link and the associated knots K_G and K_B .

Annulus twisting [38] can be odd, and sometimes has property U ; see Figure 18 and Remark 6.6. Yasui's homeomorphisms [53] are constructed such that the boundary diffeomorphism extends to a homeomorphism, hence are all even. Yasui's homeomorphism sometimes does not have property U , in fact it may never have property U ; see Section 7.3.

4. SPECIAL AND SMALL RBG LINKS

We are interested in constructing many explicit pairs K and K' with homeomorphic 0-surgeries, such that K and K' are both simple enough that we have some hope of computing their concordance invariants or constructing slice disks for them in practice. Towards these ends, in this section we collect several user-friendly results about certain subclasses of RBG links.

4.1. Special RBG links.

Definition 4.1. Let μ_R denote a meridian of R . An RBG link L is special if $b = g = 0$, $r \in \mathbb{Z}$, and there exist link isotopies

$$R \cup B \cong R \cup \mu_R \cong R \cup G.$$

Notice that for a special RBG link, $H_1(S^3_{r,b,g}(L); \mathbb{Z}) \cong \mathbb{Z}$ if and only if the determinant of the framing matrix is zero. Let l denote the linking number of B with G . Then we have

$$\begin{vmatrix} r & 1 & 1 \\ 1 & 0 & l \\ 1 & l & 0 \end{vmatrix} = 2l - rl^2 = 0.$$

Therefore, special RBG links have either $l = 0$ or $rl = 2$.

For a special RBG link, the homeomorphism $\psi_G : S^3_{r,0}(R, B) \rightarrow S^3$ is given by the slam-dunk homeomorphism of B over R . Therefore, to exhibit the knot K_G one should slide G over R until G no longer intersects the disk Δ_B bounded by B . The knot K_B can be exhibited in the same manner, everywhere reversing the roles of B and G . See Figure 3 for an example where these slides are marked and performed.

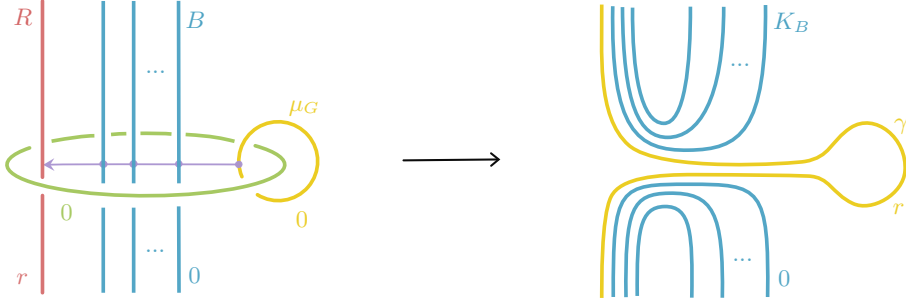


FIGURE 4. The curve γ obtained from μ_G after some handle slides and a slam-dunk.

It is easy to recognize the parity of a special RBG link:

Lemma 4.2. *A special RBG link L is even if and only if r is.*

Proof. Let $\gamma \subset S_0^3(K_B)$ be the framed knot which is the image of the 0-framed meridian of K_G under ϕ_L . Observe that $X(K_B) \cup_{\phi_L} X(-K_G)$ admits a handle decomposition given by attaching two 2-handles to B^4 along the framed link $K_B \cup \gamma$ followed by a single 4-handle. Since K_B is 0-framed and $[\gamma]$ generates $H_1(S_0^3(K_B))$, we have $lk(K_B, \gamma) = 1$. So $X(K_B) \cup_{\phi_L} X(-K_G)$ has even intersection form if and only if the framing on γ is even.

Now we will argue that γ is r -framed. First we observe that in the $S_{r,b,g}^3(R, B, G)$ surgery diagram of $S_0^3(K_G)$, the 0-framed meridian of K_G is represented by the 0-framed meridian μ_G of G . Now we will consider the framed image of this in the surgery diagram of $S_0^3(K_B)$. Observe that the image of μ_G under the slam dunk homeomorphism $S_{r,0}^3(R, G) \cong S^3$ is isotopic (as a framed curve) to the curve you get from sliding μ_G over R to clear the (single) intersection of μ_G with the disk G bounds. See Figure 4. As such, $\gamma \subset S_0^3(K_B)$ looks like the (framed) ghost of R , in particular the framing on γ is r . \square

Lemma 4.3. *If a special RBG link has $R = U$ and $r = 0$ then the associated homeomorphism has property U .*

Proof. Let L be a special RBG link and let $\gamma \subset S_0^3(K_B)$ be the framed knot given by image of the 0-framed meridian of K_G under ϕ_L . In the proof of Lemma 4.2 we argued that $\gamma \subset S_0^3(K_B)$ looks like the (framed) ghost of R , in particular γ has the knot type and framing of R . \square

Ideally, we would like to produce knots with homeomorphic zero surgeries such that exactly one of them is slice. Thus, one might like to start with their favorite slice knot K and produce a distinct knot K' with the same 0-surgery. It is not presently well-understood for which (slice) knots this is possible, but we give some lemmas that sometimes help:

Lemma 4.4 ([41] Proposition 3.2). *If K has unknotting number one then there exists a special RBG link L with K_B isotopic to K .*

Remark 4.5. In [41] it is not emphasized that the resulting RBG link is special, but one quickly checks that the proof given there does indeed produce special RBG links.

Lemma 4.6. *If K can be unknotted by performing a tangle replacement as depicted in Figure 5, then there exists a special RBG link L with K_G isotopic to K .*

Proof. In Figure 6 we demonstrate a homeomorphism from $S_0^3(K)$ to $S_{r,b,g}^3(R, B, G)$ for an RBG link L , and it is evident from the figure that K is K_G . \square

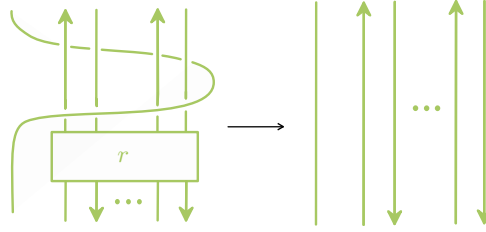
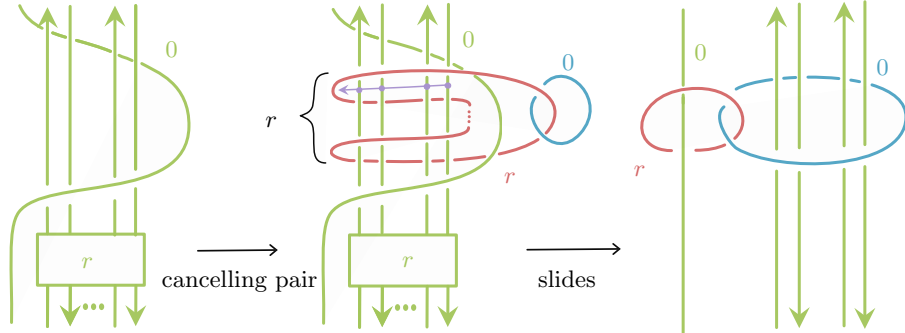
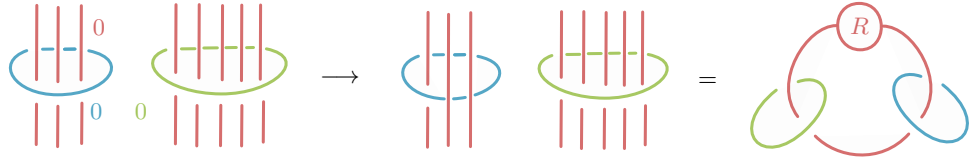


FIGURE 5. The leftmost strand may have any orientation.

FIGURE 6. A homeomorphism from $S^3_0(K)$ to surgery on an RBG link L .FIGURE 7. Crossing changes of B with R to change L (left frame) into L' (right frame).

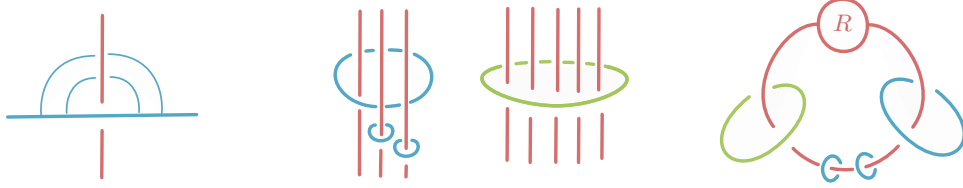
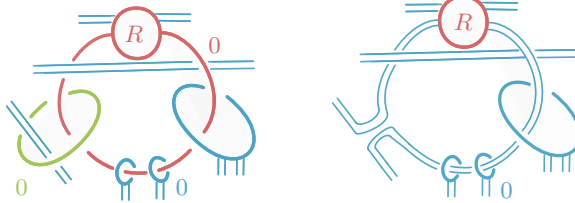
Remark 4.7. In fact, all knots can be unknotted by performing a tangle replacement as depicted in Figure 5 with $r = 0$. (This can be readily deduced from [48, Lemma 1], for example.) However when $r = 0$ one can check that the RBG link from the proof of Lemma 4.6 yields knots with $K_B = K_G$.

We now give a criterion under which special RBG links produce pairs of slice knots; for our purposes this will be a setting we will want to avoid. The following lemma is analogous to Theorem 2.3 of [41].

Lemma 4.8. *If L is a special RBG link and $B \cup G$ is split then K_B and K_G are ribbon.*

Proof. Since B and G are split, there is some sequence of crossing changes of B with R which turns L into the link $L' = R \cup \mu_R \cup \mu_R$ in the right frame of Figure 7. Each of these crossing changes can instead be exhibited by banding B to itself, as in the left frame of Figure 8, at the expense of generating an additional (blue) meridian of R . Therefore, by adding bands from the blue component to itself L can be turned into a link J' as in the right frame of Figure 8 (with some number of blue meridians). Thus we can isotope the link L into the form shown in the left frame of Figure 9; i.e. so that L looks like J' with (dual) bands connecting the blue components.

From this picture of L , we can easily cancel $G \cup R$ so that we are left with a surgery diagram of K_B ; to perform the cancellation we just first have to slide every band that geometrically links

FIGURE 8. Banding B to itself to turn L into J' (right frame).FIGURE 9. The dual bands from J' give a diagram of L from which it is easy to spot that K_B is slice.

G across R . As such, we see that K_B has a diagram of the form shown in the right frame of Figure 9. That K_B is ribbon follows from the picture. The claim that K_G is ribbon follows by symmetry of hypothesis. \square

4.2. Small RBG links.

Definition 4.9. An RBG link L is small if L is special and in addition

- B bounds a properly embedded disk Δ_B that intersects R in exactly one point, and intersects G in at most 2 points.
- G bounds a properly embedded disk Δ_G that intersects R in exactly one point, and intersects B in at most 2 points.

(All intersections are required to be transverse.)

Example 4.10. Consider the small RBG link L and associated knots K_B and K_G in Figure 3. Our natural diagrams of K_B and K_G have 20 and 16 crossings, respectively. Using SnapPy to identify the complements, we find that in fact K_B is the 12 crossing knot 12n309 and K_G is the 14 crossing knot 14n14254. To the authors' knowledge, this pair minimizes $c(K) + c(K')$ among all pairs of distinct knots with $S_0^3(K) \cong S_0^3(K')$ in the literature.

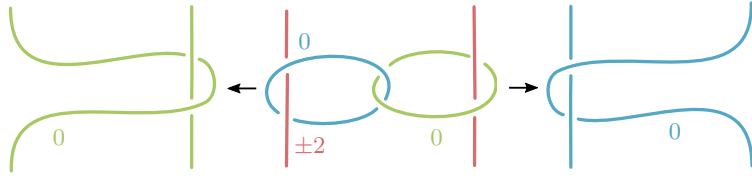
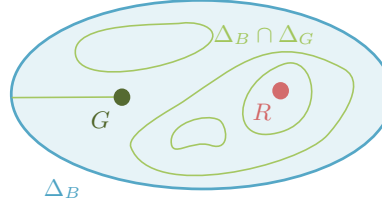
Notice that the diagrammatic conditions making a special RBG link small ensure that one only has to perform at most two slides of G over R in order to exhibit the knot K_G (resp. two slides of B over R to exhibit K_B). This helps keep the crossing number of K_G (resp. K_B) somewhat small.

In fact, for a small RBG link to produce $K_B \neq K_G$ we show that two slides are necessary.

Proposition 4.11. If L is a small RBG link with Δ_B intersecting G in less than 2 points then $K_B = K_G$.

To prove the proposition, we require two lemmas.

Lemma 4.12. Let L be a small RBG link and Δ_B and Δ_G be disks as in Definition 4.9. If $\Delta_B \cap \Delta_G$ is a single non-proper arc in each of Δ_B and Δ_G , then $K_B = K_G$.

FIGURE 10. A small RBG link with $\Delta_B \cap \Delta_G$ a single arc in each disk.FIGURE 11. The disk Δ_B for a small RBG link with $\Delta_B \cap G$ a single point.

Proof. Since we also know that both Δ_B and Δ_G intersect R in exactly one point, we can isotope L in S^3 so that a neighborhood of $\Delta_B \cup \Delta_G$ looks as in the middle frame of Figure 10. Performing the slam dunks to exhibit K_B and K_G from this picture of L yields diagrams of K_B and K_G as in the left and right frames of Figure 10; these diagrams are identical outside the neighborhood shown and isotopic inside the neighborhood shown. \square

Lemma 4.13. *Let L be a small RBG link and Δ_B and Δ_G be disks as in Definition 4.9. If $|\Delta_B \cap G| = 1$ then, after an isotopy of Δ_G rel boundary, we can arrange so that $\Delta_B \cap \Delta_G$ is as described in Lemma 4.12.*

Proof. Since Δ_B intersects G once geometrically, any disk bounded by G must intersect B once algebraically. Thus, the hypothesis that L is small implies that Δ_G intersects B exactly once geometrically.

Consider the intersection $\Delta_B \cap \Delta_G \hookrightarrow \Delta_B$; by general position this is a 1-dimensional submanifold of Δ_B (with a finite number of components, which are not necessarily properly embedded). Since $G \cap \Delta_B$ is a point, there must be exactly one arc of intersection that has exactly one endpoint in $\text{int}(\Delta_B)$. The same analysis of $\Delta_B \cap \Delta_G \hookrightarrow \Delta_G$ shows that there is exactly one arc in Δ_G that has exactly one endpoint in $\text{int}(\Delta_G)$. Endpoints of arcs in $\text{int}(\Delta_G)$ correspond to endpoints of arcs in $\partial \Delta_B$. Thus there is exactly one arc in Δ_B that has exactly one endpoint in $\partial \Delta_B$. We deduce that there is exactly one arc of intersection in Δ_B , and it has one endpoint in $\text{int}(\Delta_B)$ and one endpoint in $\partial \Delta_B$.

The other intersections are circles on Δ_B . See Figure 11. Recall that $\Delta_B \cap R = \{pt\}$, so each circle either contains $\{pt\}$ or does not. Consider an innermost circle $\gamma \subset \Delta_B$ which does not contain $\{pt\}$. Then γ bounds a disk $\Delta'_B \subset \Delta_B$ with $\Delta'_B \cap R = \emptyset$. Since γ is also a circle in Δ_G , it bounds a disk $\Delta'_G \subset \Delta_G$. Note that Δ'_G does not contain $\{pt'\} := \Delta_G \cap R$ (since if it did the disks Δ'_B and Δ'_G would give an $S^2 \leftrightarrow S^3$ with $R \cap S^2 = \{pt\}$, which is impossible for homology reasons). Thus we can replace $\Delta'_G \subset \Delta_G$ with a parallel copy of Δ'_B ; this yields a new Δ_G that has fewer circles of intersection with Δ_B . This replacement does not change the arc intersections of Δ_B with Δ_G nor the intersections of either disk with R . Continue until no such γ remain.

Now consider an innermost circle γ on Δ_B which does contain $\{pt\}$. By a similar analysis, $\gamma \subset \Delta_G$ bounds a disk $\Delta'_G \subset \Delta_G$ which does contain $\{pt'\}$. Now replacing $\Delta'_G \subset \Delta_G$ with a

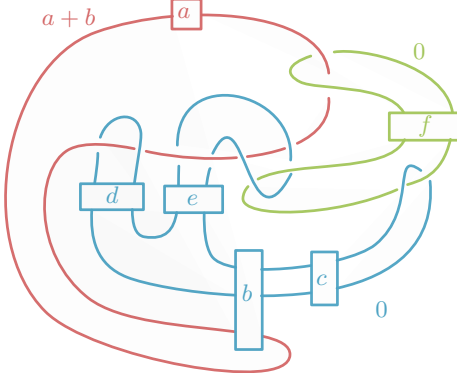


FIGURE 12. The 6-parameter RBG link which generated our 3375 examples of 0-surgery homeomorphisms.

parallel copy of Δ'_B does change $\Delta_G \cap R$, but the new $\Delta_G \cap R$ is still a single point. Continue until no such γ remain. \square

Proof of Proposition 4.11. The case that $\Delta_B \cap G$ is a single point is a consequence of Lemmas 4.13 and 4.12. In the case that $\Delta_B \cap G$ is empty, use Δ_B to isotope B to a meridian of R which does not link G . Since $R \cup G \cong R \cup \mu_G$, we can isotope $B \cup R \cup G$ to $\mu_R \cup R \cup \mu_R$. From here the slam dunk homeomorphisms give $K_B = B = U = G = K_G$. \square

Remark 4.14. When L is small and Δ_B intersects G in two points, it is possible that $\Delta_B \cap \Delta_G$ contains no circles of intersection and yet the knots K_B and K_G are distinct; the reader can check that the RBG link in Example 4.10 has this property.

In view of Proposition 4.11 (and its analogue with B and G switched), we see that if we want to produce $K_B \neq K_G$ from a small RBG link, we should only consider the cases when $|\Delta_B \cap G| = |\Delta_G \cap B| = 2$.

5. COMPUTER EXPERIMENTS

5.1. A six-parameter family of RBG links. To generate many examples of pairs of knots with the same 0-surgery, we studied the family of small RBG links shown in Figure 12. The link depends on 6 parameters (a, b, c, d, e, f) , corresponding to the numbers of full twists in each box. The first parameter a represents full twists between R and the 2-handle framing curve of R . We also have twists between R and its 2-handle framing in the box with b full twists, so overall the red curve has framing

$$r = a + b.$$

Thus, in view of Lemma 4.2, the parity of the RBG link is given by $a + b \bmod 2$.

The RBG link from Figure 12 produces the knots $K_G(a, b, c, d, e, f)$ and $K_B(a, b, c, d, e, f)$ with the same 0-surgery, as shown in Figure 13. We investigated these knots for values of the parameters ranging between -2 and 2 for the full twists on two strands, and between -1 and 1 for the full twists on four strands:

$$a, c, e \in [-2, 2], \quad b, d, e \in [-1, 1].$$

These parameters ensure that the crossing numbers of the knots K_B and K_G are at most 55.

We obtained a family of 3375 pairs of knots. We used SnapPy [13] to generate a list of these knots, compute their hyperbolic volumes, and identify some of them with knots from knot tables. Our family is sufficiently general that it includes many small knots; for example, out of the 31

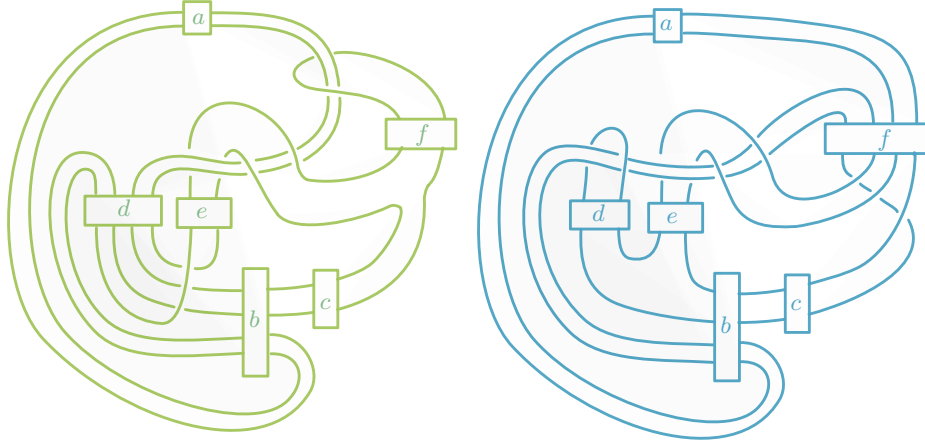


FIGURE 13. Knots $K_G(a, b, c, d, e, f)$ and $K_B(a, b, c, d, e, f)$ share a 0-surgery.

hyperbolic knots with at most 8 crossings, SnapPy recognized 19 among our data. In fact, one can show that all the knots in our family have Seifert genus at most 2 and four-ball genus at most 1; our knots include 19 of the 21 hyperbolic knots with at most 8 crossings that have these properties.

The results of our investigations are described below, and supporting files can be found online at <http://web.stanford.edu/~cm5/RBG.html>.

5.2. Methodology. We searched our list for promising pairs of knots, in particular pairs such that one knot has $s < 0$ (and therefore is not H-slice in any $\#^n \mathbb{CP}^2$), whereas the other has $s = \sigma = 0$, so has a chance of being H-slice in some $\#^n \mathbb{CP}^2$ (or perhaps even slice in B^4). (For the reason we considered $s < 0$ instead of $s > 0$, see Remark 5.3.) From the start, we could exclude some such pairs from the promising sublist using the following lemma.

Lemma 5.1. (a) If $b = -1$, then $K_G(a, b, c, d, e, f) = K_B(a, b, c, d, e, f)$.

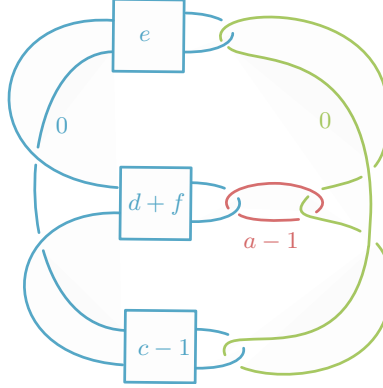
(b) If $a + b = 0$, then the knots $K_G(a, b, c, d, e, f)$ and $K_B(a, b, c, d, e, f)$ have diffeomorphic traces.

Item (b) is relevant because if the knots have diffeomorphic traces and one has $s < 0$ then the other is not slice in any $\#^n \mathbb{CP}^2$; cf. Lemma 3.5.

Proof of Lemma 5.1. (a) One can check that for $b = -1$, the RBG link from Figure 12 is isotopic to the one shown in Figure 14, which has a symmetry exchanging the B and G components. Therefore, the resulting K_B and K_G knots are isotopic.

(b) By Lemma 4.3, the fact that $r = 0$ implies that the 0-surgery homeomorphism has property U , and therefore (by Theorem 3.13) it extends to a trace diffeomorphism. \square

We then computed the signatures and the s invariants of the remaining 1800 pairs of knots. To do this, we wrote a general formula for the DT (Dowker-Thistlethwaite) codes of the knots $K_G(a, b, c, d, e, f)$ and $K_B(a, b, c, d, e, f)$, depending on the six parameters. We plugged it into *Mathematica* [52] and used the functions `KnotSignature` and `sInvariant` from the *KnotTheory`* package [7]. (Note that the signature is a 0-surgery invariant, so the signature of K_B always equals that of K_G .) For the s invariant, for some values of the parameters, the program took too long to compute (more than a few minutes). In such cases we had the option of simplifying the knot diagram in *SnapPy* with *Sage* [13, 47], using the command `K.simplify('global')`. We then plugged it back into either *KnotTheory`* or *SKnotJob* [46], where tried to decrease girth as in [18, Section 5.1] and then re-compute.

FIGURE 14. The RBG link from Figure 12, when $b = -1$.

We also used the following trick to reduce the number of knots for which we had to explicitly compute s : If we found two knots of the same type (K_B or K_G) corresponding to values (a, b, c, d, e, f) and $(a'', b'', c'', d'', e'', f'')$ with

$$a \leq a'', \quad b \leq b'', \quad c \leq c'', \quad d \leq d'', \quad e \leq e'', \quad f \leq f''$$

and with the same value of s , then we knew this value of s also holds for all the knots of the same type with intermediate values (a', b', c', d', e', f') , i.e. such that

$$a \leq a' \leq a'', \quad b \leq b' \leq b'', \quad c \leq c' \leq c'', \quad d \leq d' \leq d'', \quad e \leq e' \leq e'', \quad f \leq f' \leq f''.$$

This is a consequence of the monotonicity of the s -invariant under generalized crossing changes, which was proved in [35, Theorem 1.1].

5.3. An exclusion. As a result of our calculations, we found 24 pairs of knots with $\sigma = 0$, such that one knot in the pair has $s = 0$ and the other $s = -2$. If the knot with $s = 0$ were H-slice in $\#^n \mathbb{CP}^2$, this would produce an exotic $\#^n \mathbb{CP}^2$. For one of the 24 knots with $s = 0$, namely

$$K = K_G(0, 1, 0, -1, 2, 1)$$

we could prove that K is not H-slice in $\#^n \mathbb{CP}^2$, using the following method.

If the knot $K_G(0, 1, 0, -1, 2, 1)$ were H-slice in some $\#^n \mathbb{CP}^2$, then $K_G(-1, 1, 0, -1, 2, 1)$, which differs from it by a crossing change from negative to positive, would be H-slice in $\#^{n+1} \mathbb{CP}^2$ by Lemma 2.3. However, $K_G(-1, 1, 0, -1, 2, 1)$ has the same trace as $K_B(-1, 1, 0, -1, 2, 1)$ by Lemma 5.1(b). Therefore, $K_B(-1, 1, 0, -1, 2, 1)$ would also be H-slice in $\#^{n+1} \mathbb{CP}^2$, according to Lemma 3.5. Direct computation using *KnotTheory* gives that

$$s(K_B(-1, 1, 0, -1, 2, 1)) = -2,$$

which contradicts (1).

5.4. Interesting examples. We were left with 23 promising pairs of knots. For the knot in each pair with $s = 0$ (i.e. each candidate for being H-slice in $\#^n \mathbb{CP}^2$), we simplified the diagrams in *SnapPy* with *Sage*, using `K.simplify('global')`. The resulting diagrams are shown in Figures 22, 23 and 24. In Table 1 we list the apparent number of crossings (in the simplified diagram), volume and Alexander polynomials of these knots.

The Alexander polynomials of the knots K_1 through K_{21} (those in Figures 22 and 23) satisfy the Fox-Milnor condition, and therefore these are candidates for being slice. The last 2 knots (those in Figure 24) do not satisfy Fox-Milnor, but are still candidates for being H-slice in $\#^n \mathbb{CP}^2$.

Name	Identifier	# crossings	Volume	Alexander polynomial
K_1	$K_B(0, 1, 0, 1, 2, -1)$	29	15.451403388	1
K_2	$K_B(1, 1, -1, 1, 2, -1)$	29	16.583603453	$t^2 - 2t + 3 - 2t^{-1} + t^{-2}$
K_3	$K_B(1, 1, 0, 1, 1, -1)$	29	14.698440095	1
K_4	$K_B(1, 1, 1, 1, 0, -1)$	31	18.694759676	$t^2 - 6t + 11 - 6t^{-1} + t^{-2}$
K_5	$K_B(1, 1, 2, 1, -1, -1)$	36	21.768651216	$4t^2 - 20t + 33 - 20t^{-1} + 4t^{-2}$
K_6	$K_G(1, 1, -1, -1, 2, 1)$	32	21.917877366	$t^2 - 2t + 3 - 2t^{-1} + t^{-2}$
K_7	$K_G(1, 1, 0, -1, 1, 1)$	32	20.930658865	1
K_8	$K_G(1, 1, 1, -1, 0, 1)$	32	23.276452522	$t^2 - 6t + 11 - 6t^{-1} + t^{-2}$
K_9	$K_G(1, 1, 2, -1, -1, 1)$	41	25.720923264	$4t^2 - 20t + 33 - 20t^{-1} + 4t^{-2}$
K_{10}	$K_G(1, 1, 2, 0, -1, 1)$	20	20.032239211	$2t^2 - 12t + 21 - 12t^{-1} + 2t^{-2}$
K_{11}	$K_B(2, 1, -2, 1, 2, -1)$	35	18.623983982	$2t^2 - 6t + 9 - 6t^{-1} + 2t^{-2}$
K_{12}	$K_B(2, 1, -1, 1, 1, -1)$	29	15.552102256	1
K_{13}	$K_B(2, 1, 0, 1, 0, -1)$	31	16.662235002	$-2t + 5 - 2t^{-1}$
K_{14}	$K_B(2, 1, 1, 1, -1, -1)$	33	20.505101934	$2t^2 - 12t + 21 - 12t^{-1} + 2t^{-2}$
K_{15}	$K_B(2, 1, 2, 1, -2, -1)$	37	22.919098178	$6t^2 - 30t + 49 - 30t^{-1} + 6t^{-2}$
K_{16}	$K_G(2, 1, -2, -1, 2, 1)$	37	23.396805316	$2t^2 - 6t + 9 - 6t^{-1} + 2t^{-2}$
K_{17}	$K_G(2, 1, -2, 0, 2, 1)$	16	17.009749601	$t^2 - 2t + 3 - 2t^{-1} + t^{-2}$
K_{18}	$K_G(2, 1, -1, -1, 1, 1)$	32	21.888892554	1
K_{19}	$K_G(2, 1, 0, -1, 0, 1)$	34	22.384645541	$-2t + 5 - 2t^{-1}$
K_{20}	$K_G(2, 1, 1, -1, -1, 1)$	36	24.655381040	$2t^2 - 12t + 21 - 12t^{-1} + 2t^{-2}$
K_{21}	$K_G(2, 1, 2, -1, -2, 1)$	42	26.731842490	$2t^2 - 12t + 21 - 12t^{-1} + 2t^{-2}$
K_{22}	$K_G(2, 1, 1, 0, -1, 1)$	18	19.113083865	$t^2 - 8t + 15 - 8t^{-1} + t^{-2}$
K_{23}	$K_G(2, 1, 2, 0, -2, 1)$	22	21.642574192	$5t^2 - 26t + 43 - 26t^{-1} + 5t^{-2}$

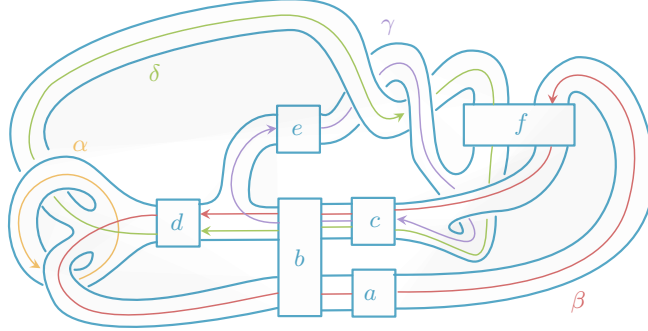
TABLE 1. Examples coming out of our computer experiments.

Proofs of Theorems 1.3 and 1.4. If K_i ($i = 1, \dots, 23$) is a knot from our list, then there is a companion knot K'_i such that $S_0^3(K) \cong S_0^3(K'_i)$ and $s(K'_i) = -2$. Therefore, K'_i is not H-slice in $\#^n \mathbb{CP}^2$ by the inequality (1). Suppose K_i were H-slice in $W = \#^n \mathbb{CP}^2$ for some n . (The case $n = 0$ corresponds to S^4 .) Then Lemma 3.3 would show that K'_i is H-slice in a 4-manifold X that is homotopy equivalent to W , and therefore homeomorphic to it by Freedman's theorem [19]. On the other hand, X could not be diffeomorphic to W , because K'_i is not H-slice in W . \square

Note that if any of the 23 knots were H-slice in $\#^n \mathbb{CP}^2$, they would actually be BPH-slice, in view of the following lemma.

Lemma 5.2. *The 23 knots in Figures 22, 23 and 24 are all H-slice in $\#^3 \overline{\mathbb{CP}^2}$.*

Proof. Observe that for all our knots, we have $b + c + e \in \{1, 2, 3\}$. When $b + c + e = 0$, the RBG link in Figure 12 has the property that its B and G components are split. By Lemma 4.8, the corresponding knots K_B and K_G (with $b + c + e = 0$) are slice. Increasing b , c or e by one corresponds to an annular cobordism in $\overline{\mathbb{CP}^2} \setminus (\dot{B}^4 \sqcup \dot{B}^4)$ between the respective knots. Therefore, if $n := b + c + e > 0$, the knots $K_B(a, b, c, d, e, f)$ and $K_G(a, b, c, d, e, f)$ are H-slice in $\#^n \overline{\mathbb{CP}^2}$. \square

FIGURE 15. A Seifert surface for the knot $K_B(a, b, c, d, e, f)$.

Remark 5.3. We also searched in our data for pairs of knots such that one has $s > 0$ and the other $s = \sigma = 0$ (which would be relevant for H-sliceness in $\#^n \mathbb{CP}^2$ instead of $\#^n \mathbb{CP}^2$), but we found no pairs of this type. Of course, we can obtain such pairs by taking the mirrors of the 23 knots in our table.

We analyzed the 23 knots from Table 1 further, to make sure they pass some well-known obstructions to being slice (or BPH-slice, as the case may be).

First, we checked that there are no algebraic obstructions coming from the Seifert matrix:

Proposition 5.4. *The 21 knots from Figures 22 and 23 are algebraically slice.*

Proof. Recall that the algebraic concordance class of a knot is given by its Seifert matrix up to S-equivalence [30, 51]. Since the Seifert matrix can be read from the 0-surgery, any two knots with the same 0-surgery are algebraically concordant. Thus, for the knots in our table of the form K_G , it suffices to check algebraic sliceness for their companions K_B .

A genus 2 Seifert surface for the knot $K_B(a, b, c, d, e, f)$ is shown in Figure 15. The associated Seifert matrix with respect to the basis $(\alpha, \beta, \gamma, \delta)$ is

$$A = \begin{pmatrix} 0 & 0 & 0 & -1 \\ 1 & a+c+d+f & c+1 & f+c+d+1 \\ 0 & c & b+c+e & b+c+1 \\ 0 & f+c+d & b+c+1 & b+c+d+f \end{pmatrix}.$$

To show that a knot $K_B(a, b, c, d, e, f)$ is algebraically slice, we will explicitly find a two-dimensional subspace V on which the Seifert form A restricts to the zero matrix. In other words, if we form a 4×2 matrix S whose columns are the basis vectors of V , we should have

$$S^T A S = 0.$$

Looking at the knots K_1 through K_{21} in Table 1, we see that with the exception of K_{10} and K_{17} , all the other values (a, b, c, d, e, f) satisfy $b = 1, d + f = 0, a + c + e = 2$. In these cases, we can take

$$V = \text{Span}\{(0, 1, 1, -1), (e - 2, 1, 0, 0)\}.$$

For K_{10} we have $(a, b, c, d, e, f) = (1, 1, 2, 0, -1, 1)$ and we choose

$$V = \text{Span}\{(2, 0, 1, -1), (2, -2, 0, 1)\}.$$

For K_{17} we have $(a, b, c, d, e, f) = (2, 1, -2, 0, 2, 1)$ and we choose

$$V = \text{Span}\{(1, 1, 1, 0), (2, 1, 0, 1)\}.$$

□

Second, for each of the 23 knots, we computed the knot Floer homology using the *Knot Floer homology calculator* [49]. The concordance invariants τ from [39], ν from [40] and ϵ from [27] vanish. As an aside, the program indicated that all the knots from our list are non-fibered, non-L-space, and have Seifert genus equal to 2.

Third, we used the program *SKnotJob* [46] to minimize the girth of the diagrams, and compute several Ramussen-type concordance invariants. Apart from the usual s (which is defined from Khovanov homology over \mathbb{Q}), the program computed $s^{\mathbb{F}_2}$ and $s^{\mathbb{F}_3}$ (from Khovanov homology over \mathbb{F}_2 and \mathbb{F}_3), as well as the Lipshitz-Sarkar s^{Sq^1} invariant (from the first Steenrod square on Khovanov homology [33]). All the knots had girth at most 10, and each calculation lasted only a few seconds. All the invariants turned out to be 0. (On the other hand, computing the Lipshitz-Sarkar $s_{\pm}^{\text{Sq}^2}$ invariants using a program such as [45] did not seem feasible, because our knots have at least 16 crossings.)

Finally, from Lemma 4.2 we see that 14 knots in Table 1 (namely, K_1 and K_{11} through K_{23}) correspond to odd RBG links, because $r = a + b$ is odd. In such a case, Theorem 3.7 shows that the 0-surgery homeomorphism relating the knot and its companion does not extend to traces. Therefore, for those 14 knots, sliceness and BPH-sliceness cannot be excluded by the fact that we have obstructed their companion knot (which we knew not to be BPH-slice because $s = -2$). Moreover, modulo the caveat in footnote¹, *SnapPy* indicates that the 0-surgeries on all our 23 knots are hyperbolic and have trivial isometry group (and hence trivial homeomorphism group, by Mostow rigidity). Hence, we expect that for the 14 examples with r odd, the trace of the knot is not even homeomorphic to that of its companion knot.

We also attempted (unsuccessfully) to show the knots are slice, or at least BPH-slice. We searched for ribbon bands using Gong's program [24], but we could not find any simple bands that produce a strongly slice link. We then tried to use Lemma 2.5 to prove BPH-sliceness, but changing any positive to a negative crossing in our diagrams resulted in knots with $\sigma = 2$, which cannot be BPH-slice. For several knots in the table, we also tried to find a slice derivative as follows: we wrote down a (genus 2) Seifert surface F for K and the associated Seifert matrix A , and then classified all dimension 2 subspaces of $H_1(F)$ on which A restricts to the 0-matrix. For each such half-basis, we drew a 2-component link $L \subset S^3$ embedded on F representing that basis; such a link is usually called a *derivative* of K . It is well known (see [30]) that if K admits a strongly slice derivative then K is slice. Unfortunately, for the handful of K for which we performed this tedious computation, none of the links L were strongly slice; this was checked using Levine-Tristram signatures or covering link calculus.

6. HOMOTOPY 4-SPHERES FROM ANNULUS TWISTING

Annulus twisting is a construction of 0-surgery homeomorphisms which stands out for its ability to naturally produce infinitely many knots with the same 0-surgery. In view of Theorem 1.2, there are RBG links associated to annulus twisting; see Section 7.2 for their description. In this section we will discuss some homotopy 4-spheres that arise from annulus twisting, without explicit reference to the corresponding RBG links.

6.1. Annulus twisting. Annulus twisting was defined by Osolinach [38], and extended to other framings and to Klein bottle twisting by Abe-Jong-Luecke-Omae [1]. Since we will need to discuss it in some detail, we reproduce the proof that annulus twisting gives rise to 0-surgery homeomorphisms.

Let $A : S^1 \times I \rightarrow S^3$ be an embedding (by the standard abuse, we will conflate the embedding and its image) and let $\ell_1 \cup \ell_2 = \partial A$ a framed oriented link in S^3 , where both the framing and the orientation are inherited from A ; when A is thought of as an oriented cobordism from $S^1 \rightarrow S^1$, we are setting $\ell_2 = \partial^+ A$. Now let γ denote a pair of pants and let $\Gamma : \gamma \rightarrow S^3$ be an embedding

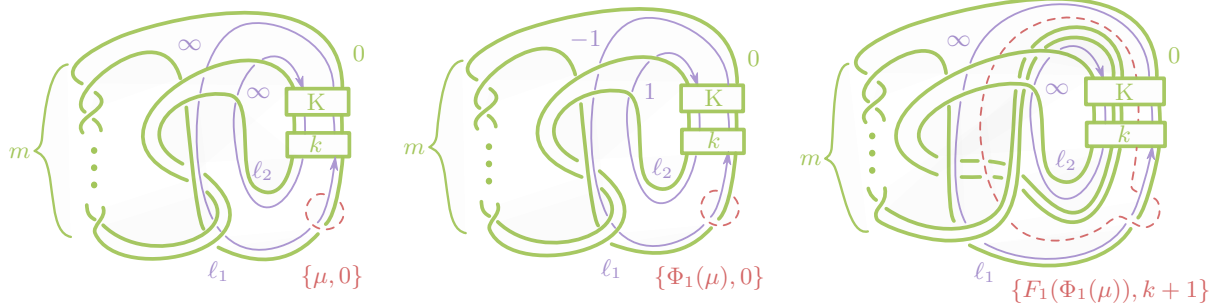


FIGURE 16. Annulus twisting a link $\ell_1 \cup \ell_2 \cup J$, with ℓ_1 and ℓ_2 drawn in purple and J in green. Here $n = 1$ and we keep track of the image of a 0-framed meridian of J under the annulus twist homeomorphism.

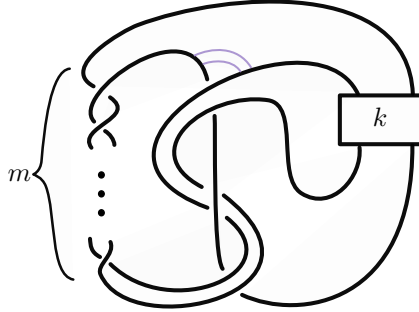


FIGURE 17. A family of knots $J_m[k]$. When $m = 3 - 2k$ the knots are ribbon, which can be seen by performing the purple band move indicated.

such that the framed oriented boundary of Γ is $\ell_1 \cup \ell_2 \cup J$ for some 0-framed knot J . We can think of J as obtained by joining a parallel copy of ℓ_1 to a parallel copy of ℓ_2 using a band. See the left hand side of Figure 16 for examples of links $\ell_1 \cup \ell_2 \cup J$; there, the K box represents parallel strands that are tied in some 0-framed knot K , and the k box represents k positive full twists. See also Figure 17 for examples of knots J that arise this way, when K is the unknot.

Theorem 6.1 (Main theorem of [38]). *Associated to such a link $\ell_1 \cup \ell_2 \cup J$ there is an infinite family of knots $(J_n)_{n \in \mathbb{Z}}$ such that $S_0^3(J_n) \cong S_0^3(J)$.*

Remark 6.2. We make no claim on the distinctness of the knots J_n here, but the interested reader should consult [5], which gives some weak conditions on $\ell_1 \cup \ell_2 \cup J$ that guarantee infinitely many of the J_n are pairwise distinct.

Proof. The proof follows from two claims: first we will show that $S_0^3(J) \cong S_{0,1/n,-1/n}^3(J, \ell_1, \ell_2)$. Second we will define J_n and show that $S_{0,1/n,-1/n}^3(J, \ell_1, \ell_2) \cong S_0^3(J_n)$. We remark that these surgery coefficients are relative to the given framing (which often differs from the Seifert framing).

Towards the first claim, observe that in $S_0^3(J)$ the pair of pants Γ can be capped off with the surgery disk to give an embedded annulus Γ' with framed oriented boundary $\ell_1 \cup \ell_2 \subset S_0^3(J)$. We'll use Γ' to define a homeomorphism

$$\Phi_n : S_0^3(J) \rightarrow S_{0,1/n,-1/n}^3(J, \ell_1, \ell_2)$$

as follows. Consider $Y = S_0^3(J) \setminus \nu(\ell_1 \cup \ell_2)$ and observe that Γ' restricts to a properly embedded annulus in Y . Consider $\nu(\Gamma') \cong S^1 \times I \times I$, where the final I factor comes from the normal

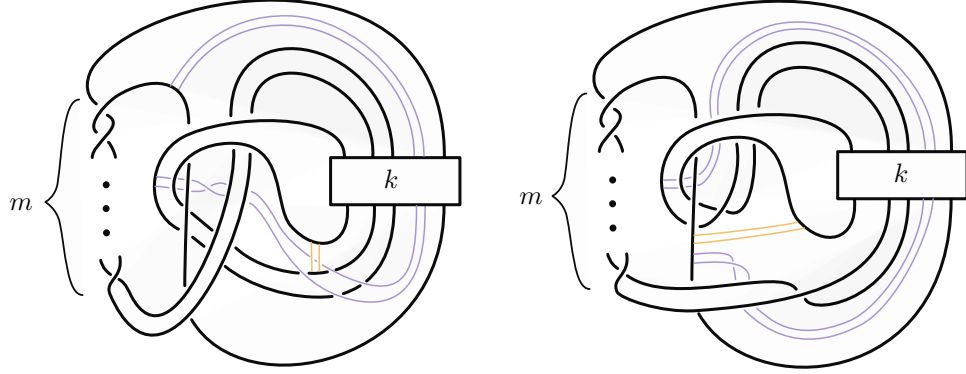


FIGURE 18. The knots $J_m[k]_1$ and $J_m[k]_{-1}$ obtained from the knots in Figure 17 by annulus twisting. When $m = 3 - 2k$ the knots are ribbon, which can be seen by performing the purple and yellow band moves indicated.

direction. Define the homeomorphism

$$\phi_n : S^1 \times I \times I \rightarrow S^1 \times I \times I, \quad \phi_n(\theta, x, t) = (\theta + n(2\pi i)t, x, t).$$

Since $\phi_n|_{S^1 \times I \times \partial I}$ is the identity map, we can extend ϕ_n to a self homeomorphism Φ_n of Y by taking the identity map outside of $\nu(\Gamma')$.

We will now extend Φ_n to a homeomorphism with domain $S^3_0(J)$. We can do this by simply reattaching the excised neighborhoods $\nu(\ell_1 \cup \ell_2)$, but in the target space we must take care to reattach along the gluing map modified by Φ_n . We see that $\Phi_n|_{\partial Y}$ takes the meridional curve in $\partial(\nu(\ell_1))$ (resp. $\partial(\nu(\ell_2))$) to the $\frac{1}{n}$ curve on $\partial(\nu(\ell_1))$ (resp. $\frac{-1}{n}$ curve on $\partial(\nu(\ell_2))$). Thus the first claim follows.

To prove the second claim, observe that by hypothesis $\ell_1 \cup \ell_2$ cobound an annulus A in S^3 . We can twist S^3 along A as in the proof of the first claim to produce a homeomorphism

$$f_n : S^3_{1/n, -1/n}(\ell_1 \cup \ell_2) \rightarrow S^3.$$

Since the knot $\iota_n(J) \subset S^3_{1/n, -1/n}(\ell_1 \cup \ell_2)$ (where the embedding ι_n is given by any diagram of $J \cup \ell_1 \cup \ell_2$) may intersect A , the image $f_n(\iota_n(J))$ is some a priori new knot $J_n \subset S^3$. Surgering on $\iota_n(J)$ and its image under f_n , we get a homeomorphism

$$F_n : S^3_{0,1/n, -1/n}(J, \ell_1, \ell_2) \rightarrow S^3_{r_n}(J_n).$$

In general one would now need to inspect f_n to compute r_n , but since $H_1(S^3_{0,1/n, -1/n}(J, \ell_1, \ell_2)) \cong \mathbb{Z}$ we can conclude $r_n = 0$. \square

6.2. Examples. Consider the family of knots $J_m[k]$ pictured in Figure 17. (When $k = 1$, this recovers the family J_m from [2, Figure 4].) We ask for m to be odd but we allow it to be negative—in which case we have $|m|$ left-hand half twists in the picture. Similarly, we allow the number k of full twists on the right to be an arbitrary integer. In all figures we are taking the annulus $A \cong S^1 \times I$ to be oriented such that the S^1 factor is counterclockwise in the figure and the I factor points radially inward. For this orientation of A , ℓ_2 is the oriented curve marked in Figure 16 and in the standard orientation of S^3 , the normal direction t to A points into the page.

Annulus twisting applied to each $J = J_m[k]$ (with ℓ_1 and ℓ_2 as in Figure 20) produces an infinite family of knots, $J_m[k]_n$, with the same 0-surgeries as we vary n . Of these, we show $J_m[k]_1$ and $J_m[k]_{-1}$ in Figure 18.

$m \backslash k$	-2	-1	0	1	2	3
-5	(2, 2)	(2, 2)	(0, 0)	(0, 0)	(0, 0)	(0, 0)
-3	(2, 2)	(2, 2)	(0, 0)	(0, 0)	(0, 0)	(0, 0)
-1	(2, 2)	(2, 2)	(0, 0)	(0, 0)	(0, 0)	(0, 0)
1	(2, 0)	(2, 0)	(0, 0)	(0, 0)	(0, 0)	(0, 0)
3	(2, 0)	(2, 0)	(0, 0)	(0, -2)	(0, -2)	(0, -2)
5	(0, 0)	(0, 0)	(0, 0)	(0, -2)	(0, -2)	(0, -2)
7	(0, 0)	(0, 0)	(0, 0)	(-2, -2)	(-2, -2)	(-2, -2)

TABLE 2. Values of (σ, s) for knots of the form $J_m[k]$.

As in Section 5, in the hope of producing an exotic S^4 or $\#^n \mathbb{CP}^2$, we looked for examples where one of the $J_m[k]$ and $J_m[k]_{\pm 1}$ was slice (or H-slice in $\#^n \mathbb{CP}^2$), and another was not. For this, we would like that the knots satisfy $\sigma = 0$, and the values of the s invariant are different.

Observe that if $k = 0$, then $J_m[k]$ and $J_m[k]_{\pm 1}$ are unknotted. Furthermore, when $k = \pm 1$, the knots $J_m[k]$ and $J_m[k]_{\pm 1}$ share the same trace; this was originally proven in [2, Theorem 2.8]; the readers can see this for themselves as a consequence of Theorem 3.13 and Remark 6.6. Thus, in view of Lemma 3.5, the only hope for interesting examples comes from the cases $|k| \geq 2$. As noted in Remark 6.6, for the annulus knots in Figure 17, the homeomorphism coming from twisting $J_m[k]$ once in either direction is odd if and only if k is even, so the setting $k = 2$ should generically yield knots which do not have homeomorphic traces.

Unfortunately, we found no examples with $\sigma = 0$ and different s for small values of k and m . Table 2 displays the values of the pair (σ, s) for $J_m[k]$. For all the knots in the table except the one marked in blue, namely $J_1[-2] = 11n79$, the value of s stays the same when we do annulus twisting in either direction. For $J_1[-2]$, we have $s = 0$ but both annulus twists, $J_1[-2]_1$ and $J_1[-2]_{-1}$, have $s = 2$ instead of $s = 0$. (However, the signature is nonzero in this example.)

A few remarks are in order about the knots in Table 2. We marked in red those knots where we know that the knot and its annulus twists are slice. For the knots $J_{3-2k}[k]$ and their annulus twists, Figures 17 and 18 show the existence of ribbon bands relating them to the unlink. Note that many of these (untwisted) examples can be recognized from knot tables. Indeed, we have:

$$J_5[-1] = 13n469, \quad J_3[0] = \text{unknot}, \quad J_1[1] = 820, \quad J_{-1}[2] = 88, \quad J_{-3}[3] = 13n1209.$$

Observe also that all knots between the vertical unknot line and the diagonal slice line (that is, $J_m[k]$ with $k \geq 0, m \leq 3 - 2k$ or $k \leq 0, m \geq 3 - 2k$) are BPH-slice, and so are their annulus twists. This is because we can get from them to a slice knot by changing crossings in either direction; cf. Lemma 2.5.

Remark 6.3. The knots $J_{-1}[2] = 88$ and $J_{-1}[2]_1$ appear in the list considered in Section 5, as $K_G(2, 1, 0, 0, 1, -1)$ and $K_B(2, 1, 0, 0, 1, -1)$. Furthermore, the knots $J_{-1}[2] = 88$ and $J_{-1}[2]_{-1}$ appear in the list as $K_G(-1, 0, -2, 1, 0, 1)$ and $K_B(-1, 0, -2, 1, 0, 1)$; and also as $K_G(1, 0, 0, 0, 2, -1)$ and $K_B(1, 0, 0, 0, 2, -1)$.

6.3. Homotopy 4-spheres. Suppose that K is a slice knot, and that K and K' admit a 0-surgery homeomorphism $\phi : S_0^3(K) \rightarrow S_0^3(K')$. As in the proof of Lemma 3.3, we can construct

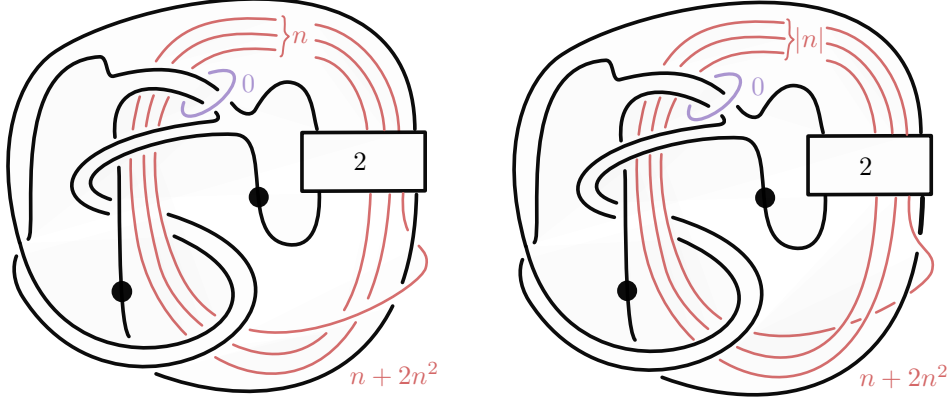


FIGURE 19. Homotopy spheres associated to annulus twisting 8_8 . Left $n > 0$, right $n < 0$.

the homotopy 4-sphere

$$X = X(-K') \cup_{\phi} V,$$

where V is any slice disk exterior for K . Even when we know that both K and K' are slice, it is not clear that X is a standard 4-sphere. We present below some examples of such homotopy 4-spheres, for which we could not verify that X is S^4 .

Example 6.4. We first give examples coming from the knot $K = J_{-1}[2] = 8_8$ and K' any of its annulus twists. The knot 8_8 is slice, we have exhibited a ribbon band, and hence ribbon disk D , in Figure 17. To draw a handle decomposition of $V = B^4 \setminus \nu(D)$ we use the rising water principle; see [23, Chapter 6.2]. This decomposition is given by the black and purple curves in Figure 19.

As argued in the proof of Lemma 3.3, X has a handle diagram obtained from that of V by adding an additional 0-framed 2-handle along $\phi^{-1}(\mu_{K'})$, followed by a 4-handle. In Figure 16 we give an example identification of the framed curve $\phi^{-1}(\mu_{K'})$ in $S_0^3(K)$, where ϕ is the homeomorphism given by annulus twisting $J_m(k)$ once and $\mu(K')$ is 0-framed. In Figure 19 we exhibit in red the framed curve $\phi_n^{-1}(\mu_{K'}) \subset \partial V$ where ϕ_n is the homeomorphism given by annulus twisting 8_8 n times, for $n \neq 0$. These images are computed by inspection of the annulus twist homeomorphism, which we gave explicitly in the proof of Theorem 6.1.

Remark 6.5. Kyle Hayden informed us that for $n = 1$, the homotopy 4-sphere shown in Figure 19 is standard.

Remark 6.6. By keeping track of the image of a meridian as we have done in Figure 16, it is straightforward to check that annulus twisting once in either direction is even if and only if k is odd, and that annulus twisting has property U when $K = U$ and $k = \pm 1$.

7. CONNECTIONS WITH OTHER CONSTRUCTIONS

In this section we draw RBG links for some of the 0-surgery homeomorphisms in the literature. Theoretically, there is no work to this; the procedure to draw an RBG link for a fixed homeomorphism is given in the proof of Theorem 1.2. However, we find the pictures to be a helpful reference, thus we include them here. We have also made some effort to give particularly elegant RBG links where possible.

Some relationships between annulus twisting, the methods in [41], and dualizable patterns have already been illustrated in the literature; see [36, 41, 50].

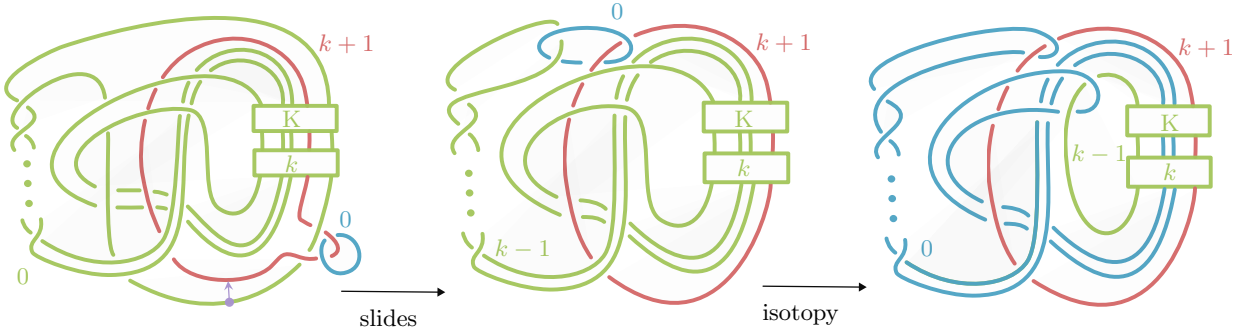


FIGURE 20. Simplifying an RBG link for annulus twisting.

7.1. Preliminaries. Recall that Dehn surgery diagrams can be modified by “handle sliding” without changing the homeomorphism type of the manifold described. We observe now that certain handle slides of RBG links are RBG preserving; this proposition will allow us to draw particularly nice RBG links for some constructions.

Proposition 7.1. *Let L be an RBG link and L' be a framed link obtained from L by some number of slides of B over R . Then L' is an RBG link and the pair of knots K'_B and K'_G associated to L' are pairwise isotopic to the pair of knots K_B and K_G associated to L .*

Remark 7.2. By symmetry of the RBG construction, the proposition also holds with the roles of B and G reversed.

Proof. First we check that L' is an RBG link. Since R and G are unchanged, the framed link $G \cup R$ still surgers to S^3 . Since the framed link $B \cup R$ surgered to S^3 before the slides, the framed link $B' \cup R$ surgers to S^3 . Finally observe that handle slides preserve the homeomorphism type, hence homology type, of the resulting manifold.

To check that $K_B \cong K'_B$ we will exhibit a homeomorphism from $S^3_0(K_B)$ to $S^3_0(K'_B)$ which carries a 0-framed meridian to a 0-framed meridian. By excising these meridians, we observe that there is a homeomorphism from $S^3 \setminus \nu(K_B)$ to $S^3 \setminus \nu(K'_B)$ taking meridians to meridians. It follows that there is a homeomorphism of pairs $(S^3, K_B) \rightarrow (S^3, K'_B)$, hence that the knots are isotopic. We will show that $K_G \cong K'_G$ in the same manner.

To define our homeomorphism $S^3_0(K_B) \rightarrow S^3_0(K'_B)$ recall that the RBG construction comes equipped with homeomorphisms $\psi_B : S^3_{r,b,g}(L) \rightarrow S^3_0(K_B)$ and $\psi'_B : S^3_{r,b',g}(L') \rightarrow S^3_0(K'_B)$. Let $f : S^3_{r,b,g}(L) \rightarrow S^3_{r,b',g}(L')$ the slide homeomorphism, and consider $\psi'_B \circ f \circ (\psi_B)^{-1} : S^3_0(K_B) \rightarrow S^3_0(K'_B)$. Now we'll watch a 0-framed meridian of K_B under each leg of the map: under $(\psi_B)^{-1}$ it goes to a 0-framed meridian of B , under f to a 0-framed meridian of B' , and under ψ'_B to a 0-framed meridian of K'_B . The construction and meridian-watching for G is similar and left to the reader. \square

7.2. Annulus twisting. To draw an RBG link for annulus twisting we follow the process outlined in the proof of Theorem 1.2. In Figure 20 we have carried a (red) 0-framed meridian of K through the homeomorphism to $S^3_0(J_1)$. Here the framing label on red is in terms of the usual convention, i.e. with respect to the diagrammatic Seifert framing. Thus we obtain an RBG link for annulus twisting from the left hand frame of Figure 20 by adding a blue 0-framed meridian to the red curve.

By Proposition 7.1, we can modify this RBG by slides of B or G over R as we like. We exhibit a particularly simple RBG link by considering the slide and isotopy shown in Figure 20. We remark that if K is non-trivial or $k \neq \pm 1$, then this RBG link is not special.

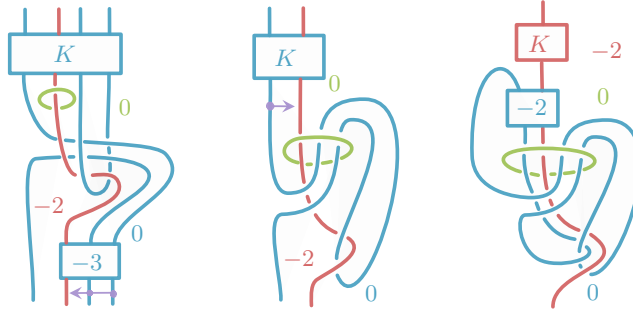


FIGURE 21. Braid closures of these tangles give RBG links for Yasui's homeomorphism.

7.3. Yasui's construction. In [53] Yasui gives a construction of knots with homeomorphic 0-surgeries which he uses to disprove the Akbulut-Kirby conjecture. While we enthusiastically recommend his paper, in fact we will model our diagrams off of the (reproduced) proof of his construction given in Section 2.1 of [25].

We restrict to the $n = 0$ setting and consider a (red) 0-framed meridian of the green curve in Figure 3(a) of [25]. We then inspect the image of that red meridian under the handle calculus in Figure 3 of [25]. Part (h) of that figure, together with image of the red curve, and a green 0-framed meridian of that red image, is the first frame of our Figure 21. (We remark that the calculus described in Figure 3 of [25] is local; the knot $K \subset \partial Z$ used in their Proposition 2.2 can go wherever it wants outside of the region shown in their Figure 3. Our Figure 21 is global and our $Z \cong B^4$; thus we depict that K may be knotted with the region marked K in Figure 21.) Appealing to Proposition 7.1, we can tidy up this RBG link via the slides and isotopy marked in Figure 21 to obtain the rather nice simple RBG link in the right frame of Figure 21.

7.4. Dualizable patterns. The dualizable patterns technique was developed and utilized in [3, 32, 9, 22, 6, 36]. In [41] an early version of the RBG construction was developed; in [41] an RBG link is required to have $r = 0$, $B \cup R = B \cup \mu_B$, $G \cup R = G \cup \mu_G$ and $lk(B, G) = 0$. (We remark that the RBG links studied there have property U , but are not necessarily special.) In the appendix to [41], it is proven that any homeomorphism constructed by the dualizable patterns technique may be presented by an RBG link of the type studied in [41] and the converse: any RBG link of that type gives rise to a dualizable pattern. Instead of including a reproof here, which would require recalling the dualizable patterns construction, we refer the reader to the appendix of that paper.

REFERENCES

- [1] T. Abe, I. D. Jong, J. Luecke, and J. Osolinach, *Infinitely many knots admitting the same integer surgery and a four-dimensional extension*, Int. Math. Res. Not. IMRN, (2015), no. 22, 11667–11693.
- [2] T. Abe, I. D. Jong, Y. Omae, and M. Takeuchi, *Annulus twist and diffeomorphic 4-manifolds*, preprint, arXiv:1209.0361, 2012.
- [3] S. Akbulut, *On 2-dimensional homology classes of 4-manifolds*, Math. Proc. Cambridge Philos. Soc., **82**(1977), no. 1, 99–106.
- [4] S. Akbulut, *Cappell-Shaneson homotopy spheres are standard*, Ann. of Math. (2), **171**(2010), no. 3, 2171–2175.
- [5] K. L. Baker, C. Gordon, and J. Luecke, *Bridge number and integral Dehn surgery*, Algebr. Geom. Topol., **16**(2016), no. 1, 1–40.
- [6] K. L. Baker and K. Motegi, *Noncharacterizing slopes for hyperbolic knots*, Algebr. Geom. Topol., **18**(2018), no. 3, 1461–1480.

- [7] D. Bar-Natan and S. Morrison, *The Mathematica package KnotTheory*, available at <http://katlas.org/wiki/KnotTheory>.
- [8] S. Boyer, *Simply-connected 4-manifolds with a given boundary*, Trans. Amer. Math. Soc., **298**(1986), no. 1, 331–357.
- [9] W. R. Brakes, *Manifolds with multiple knot-surgery descriptions*, Math. Proc. Cambridge Philos. Soc., **87**(1980), no. 3, 443–448.
- [10] J. Cerf, *Sur les difféomorphismes de la sphère de dimension trois ($\Gamma_4 = 0$)*, Lecture Notes in Mathematics, No. 53, Springer-Verlag, Berlin-New York, 1968.
- [11] T. D. Cochran, S. Harvey, and P. Horn, *Filtering smooth concordance classes of topologically slice knots*, Geom. Topol., **17**(2013), no. 4, 2103–2162.
- [12] T. D. Cochran and E. Tweedy, *Positive links*, Algebr. Geom. Topol., **14**(2014), no. 4, 2259–2298.
- [13] M. Culler, N. M. Dunfield, M. Goerner, and J. R. Weeks, *SnapPy, a computer program for studying the geometry and topology of 3-manifolds*, available at <http://snappy.computop.org>.
- [14] A. Daemi and C. Scaduto, *Chern-Simons functional, singular instantons, and the four-dimensional clasp number*, preprint, arXiv:2007.13160, 2020.
- [15] S. K. Donaldson, *An application of gauge theory to four-dimensional topology*, J. Differential Geom., **18**(1983), no. 2, 279–315.
- [16] N. M. Dunfield, N. R. Hoffman, and J. E. Licata, *Asymmetric hyperbolic L -spaces, Heegaard genus, and Dehn filling*, Math. Res. Lett., **22**(2015), no. 6, 1679–1698.
- [17] R. H. Fox and J. W. Milnor, *Singularities of 2-spheres in 4-space and cobordism of knots*, Osaka Math. J., **3**(1966), 257–267.
- [18] M. Freedman, R. Gompf, S. Morrison, and K. Walker, *Man and machine thinking about the smooth 4-dimensional Poincaré conjecture*, Quantum Topol., **1**(2010), no. 2, 171–208.
- [19] M. H. Freedman, *The topology of four-dimensional manifolds*, J. Differential Geom., **17**(1982), no. 3, 357–453.
- [20] D. Gabai, *Foliations and the topology of 3-manifolds*, Bull. Amer. Math. Soc. (N.S.), **8**(1983), no. 1, 77–80.
- [21] H. Gluck, *The embedding of two-spheres in the four-sphere*, Trans. Amer. Math. Soc., **104**(1962), 308–333.
- [22] R. E. Gompf and K. Miyazaki, *Some well-disguised ribbon knots*, Topology Appl., **64**(1995), no. 2, 117–131.
- [23] R. E. Gompf and A. I. Stipsicz, *4-manifolds and Kirby calculus*, volume 20 of *Graduate Studies in Mathematics*, American Mathematical Society, Providence, RI, 1999.
- [24] S. Gong, *Adding bands*, software, available at <https://www.math.ucla.edu/~sgongli/code.html>.
- [25] K. Hayden, T. E. Mark, and L. Piccirillo, *Exotic Mazur manifolds and knot trace invariants*, preprint, arXiv:1908.05269, 2019.
- [26] K. Hayden and L. Piccirillo, *The trace embedding lemma and spinelessness*, preprint, arXiv:1912.13021, 2019.
- [27] J. Hom, *Bordered Heegaard Floer homology and the tau-invariant of cable knots*, J. Topol., **7**(2014), no. 2, 287–326.
- [28] N. Iida, A. Mukherjee, and M. Taniguchi, *An adjunction inequality for Bauer Furuta type invariants, with applications to sliceness and 4-manifold topology*, preprint, arXiv:2102.02076, 2021.
- [29] P. B. Kronheimer and T. S. Mrowka, *Gauge theory and Rasmussen's invariant*, J. Topol., **6**(2013), no. 3, 659–674, corrigendum available at [arxiv:1110.1297v3](https://arxiv.org/abs/1110.1297v3).
- [30] J. Levine, *Invariants of knot cobordism*, Invent. Math., **8**(1969), 98–110; addendum, ibid. **8** (1969), 355.
- [31] W. B. R. Lickorish, *Surgery on knots*, Proc. Amer. Math. Soc., **60**(1976), 296–298 (1977).
- [32] W. B. R. Lickorish, *Shake-slice knots*, in *Topology of low-dimensional manifolds (Proc. Second Sussex Conf., Chelwood Gate, 1977)*, Springer, Berlin, volume 722 of *Lecture Notes in Math.*, pp. 67–70, 1979.
- [33] R. Lipshitz and S. Sarkar, *A refinement of Rasmussen's S -invariant*, Duke Math. J., **163**(2014), no. 5, 923–952.
- [34] C. Manolescu, M. Marengon, and L. Piccirillo, *Relative genus bounds in indefinite four-manifolds*, preprint, arXiv:2012.12270, 2020.
- [35] C. Manolescu, M. Marengon, S. Sarkar, and M. Willis, *A generalization of Rasmussen's invariant, with applications to surfaces in some four-manifolds*, preprint, arXiv:1910.08195, 2019.
- [36] A. N. Miller and L. Piccirillo, *Knot traces and concordance*, J. Topol., **11**(2018), no. 1, 201–220.
- [37] J. Milnor and D. Husemoller, *Symmetric bilinear forms*, Springer-Verlag, New York-Heidelberg, ergebnisse der Mathematik und ihrer Grenzgebiete, Band 73, 1973.
- [38] J. K. Osoinach, Jr., *Manifolds obtained by surgery on an infinite number of knots in S^3* , Topology, **45**(2006), no. 4, 725–733.
- [39] P. Ozsváth and Z. Szabó, *Knot Floer homology and the four-ball genus*, Geom. Topol., **7**(2003), 615–639.
- [40] P. S. Ozsváth and Z. Szabó, *Knot Floer homology and rational surgeries*, Algebr. Geom. Topol., **11**(2011), no. 1, 1–68.

- [41] L. Piccirillo, *Shake genus and slice genus*, Geom. Topol., **23**(2019), no. 5, 2665–2684.
- [42] L. Piccirillo, *The Conway knot is not slice*, Ann. of Math. (2), **191**(2020), no. 2, 581–591.
- [43] J. Rasmussen, *Khovanov homology and the slice genus*, Invent. Math., **182**(2010), no. 2, 419–447.
- [44] R. A. Robertello, *An invariant of knot cobordism*, Comm. Pure Appl. Math., **18**(1965), 543–555.
- [45] S. Sarkar, *newSInvariants*, software, available at <https://www.math.ucla.edu/~sucharit/programs/newSInvariants>.
- [46] D. Schütz, *SKnotJob*, software, available at <http://www.maths.dur.ac.uk/~dma0ds/knotjob.html>.
- [47] W. Stein *et al.*, *Sage Mathematics Software (Version 9.2)*, The Sage Development Team, available at <http://www.sagemath.org>, 2020.
- [48] S. Suzuki, *Local knots of 2-spheres in 4-manifolds*, Proc. Japan Acad., **45**(1969), 34–38.
- [49] Z. Szabó, *Knot Floer homology calculator*, software, available at <https://web.math.princeton.edu/~szabo/HFKcalc.html>.
- [50] K. Tagami, *Notes on constructions of knots with the same trace*, preprint, arXiv:2010.13292, 2020.
- [51] H. F. Trotter, *On S -equivalence of Seifert matrices*, Invent. Math., **20**(1973), 173–207.
- [52] Wolfram Research, Inc., *Mathematica, Version 11.0*, URL <https://www.wolfram.com/mathematica>, Champaign, IL, 2016.
- [53] K. Yasui, *Corks, exotic 4-manifolds and knot concordance*, preprint, arXiv:1505.02551, 2015.

DEPARTMENT OF MATHEMATICS, STANFORD UNIVERSITY, STANFORD, CA 94305

Email address: cm5@stanford.edu

DEPARTMENT OF MATHEMATICS, MASSACHUSETTS INSTITUTE OF TECHNOLOGY, CAMBRIDGE, MA 02139

Email address: piccirli@mit.edu

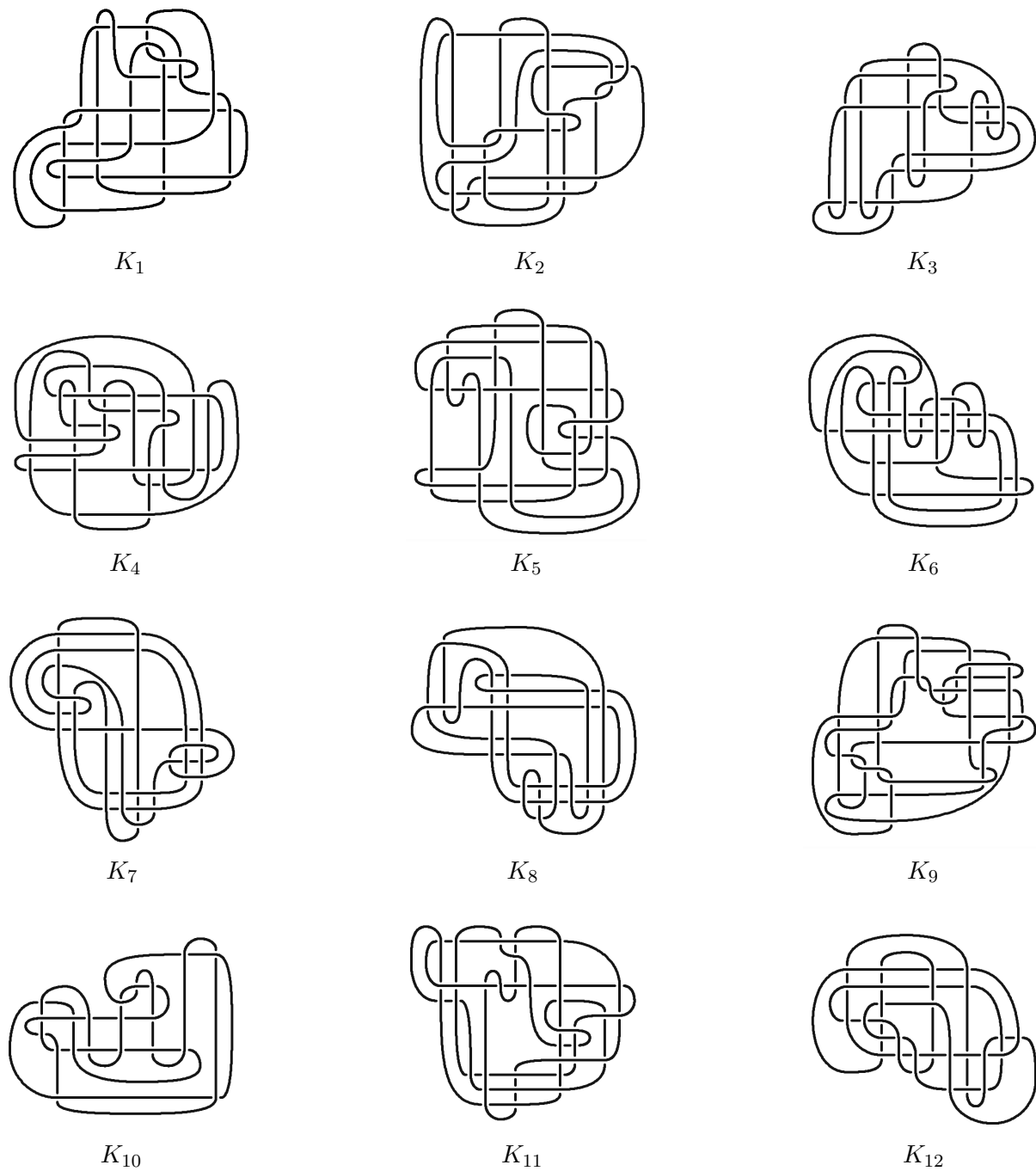


FIGURE 22. Candidates for slice knots.

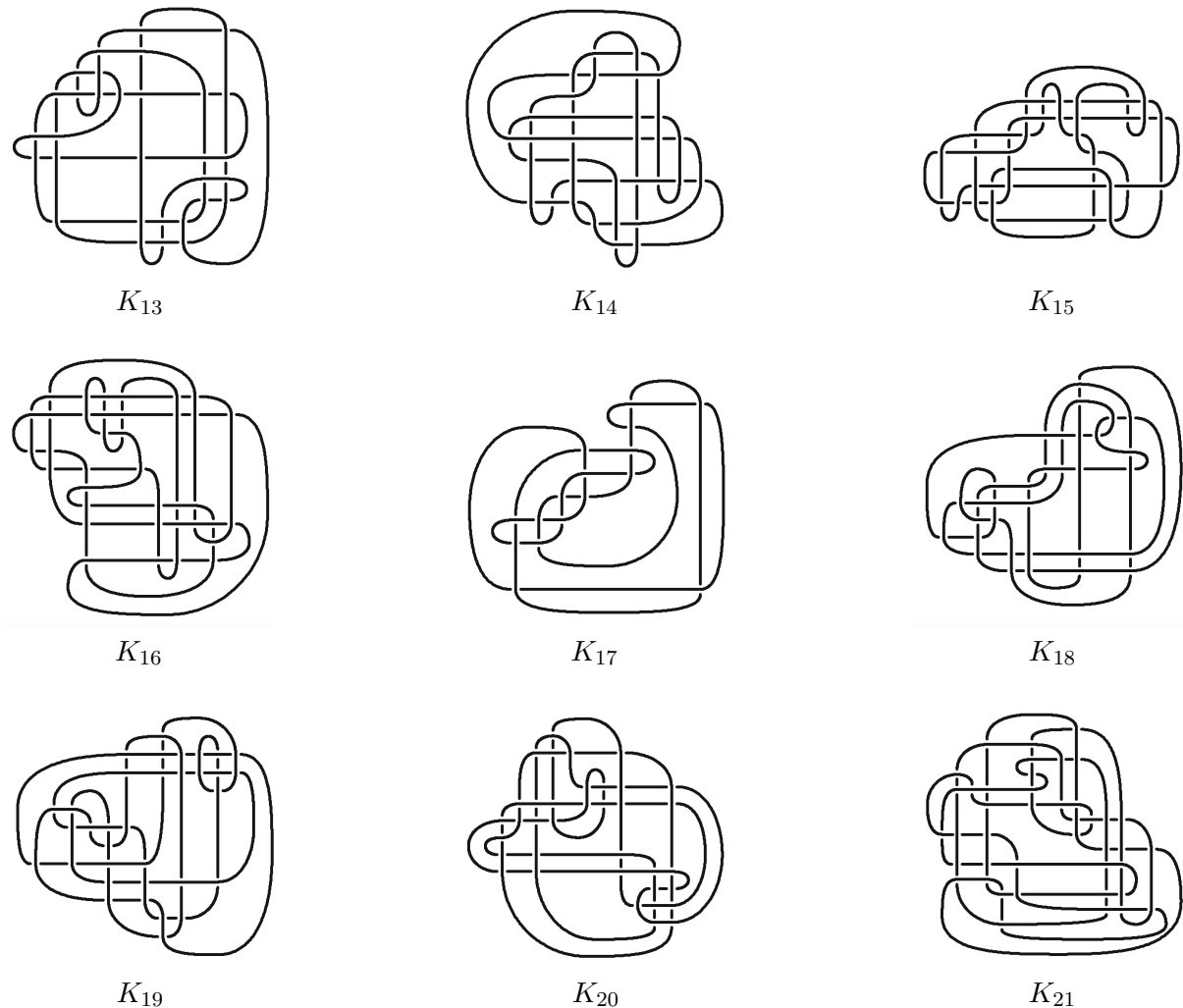


FIGURE 23. More candidates for slice knots.

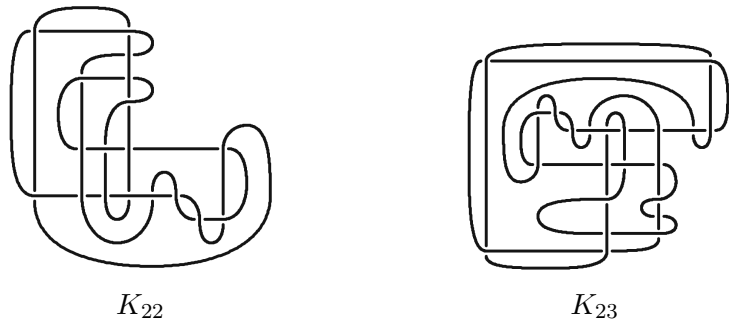


FIGURE 24. Candidates for BPH-slice knots.